© 2021. Published by The Company of Biologists Ltd | Journal of Cell Science (2021) 134, jcs258574. doi:10.1242/jcs.258574

TOOLS AND RESOURCES

A robust and flexible CRISPR/Cas9-based system for neutrophil-specific gene inactivation in zebrafish

Yueyang Wang[1,§], Alan Y. Hsu[1,*,§], Eric M. Walton[2], Sung Jun Park[3], Ramizah Syahirah[1], Tianqi Wang[1], Wenqing Zhou[1,‡], Chang Ding[1], Abby Pei Lemke[1], GuangJun Zhang[3,4,5,6], David M. Tobin[2] and Qing Deng[1,4,5,¶]

ABSTRACT

CRISPR/Cas9-based tissue-specific knockout techniques are essential for probing the functions of genes in embryonic development and disease using zebrafish. However, the lack of capacity to perform gene-specific rescue or live imaging in the tissue-specific knockout background has limited the utility of this approach. Here, we report a robust and flexible gateway system for tissue-specific gene inactivation in neutrophils. Using a transgenic fish line with neutrophil-restricted expression of Cas9 and ubiquitous expression of single guide (sg)RNAs targeting *rac2*, specific disruption of the *rac2* gene in neutrophils is achieved. Transient expression of sgRNAs targeting *rac2* or *cdk2* in the neutrophil-restricted Cas9 line also results in significantly decreased cell motility. Re-expressing sgRNA-resistant *rac2* or *cdk2* genes restores neutrophil motility in the corresponding knockout background. Moreover, active Rac and force-bearing F-actins localize to both the cell front and the contracting tail during neutrophil interstitial migration in an oscillating fashion that is disrupted when *rac2* is knocked out. Together, our work provides a potent tool that can be used to advance the utility of zebrafish in identifying and characterizing gene functions in a tissue-specific manner.

KEY WORDS: Actin stress, Cell migration, Leukocytes, Live imaging, Rac2

INTRODUCTION

Over the past decade, zebrafish (*Danio rerio*) has gained popularity as a vertebrate model organism for biological and biomedical studies, including neutrophil biology (Deng and Huttenlocher, 2012). Transparent embryos, a short life cycle (Driever et al., 1994), a highly conserved innate immune system (Lieschke and Trede, 2009), as well as ease of genetic manipulation (Lawson and Wolfe, 2011), allow for the dissection of mechanisms regulating neutrophil migration using both genetics and non-invasive high-resolution intravital imaging approaches.

In general, generating tissue-specific knockouts is essential to delineate the function of genes-of-interest in different cells and tissues. However, this technique is not sufficiently developed in the zebrafish model. The Cre/loxP site-specific recombination technology is one of the earliest conditional gene modification approaches (Hoess and Abremski, 1985) and is widely applied in mice (Branda and Dymecki, 2004). The first Cre/loxP system in zebrafish was developed in 2004, by injecting *Cre* RNA into embryos of a floxed *gfp* transgenic line (Dong and Stuart, 2004). Indeed, several studies demonstrated the feasibility of using the Cre/loxP system for tissue-specific gene inactivation in zebrafish (Cantù et al., 2018; Hans et al., 2009; Langenau et al., 2005; Pan et al., 2005; Thummel et al., 2005; Xiong et al., 2013). However, making floxed alleles at the endogenous loci is technically challenging and time consuming. A recent advance in generating the conditional allele could expand its utility in the future (Li et al., 2019a). Meanwhile, the gene-silencing approach using RNAi has only been shown to be successful in limited circumstances (de Rienzo et al., 2012; Dong et al., 2009; Kelly and Hurlstone, 2011), possibly due to a lack of reliable methods to express small interfering RNAs in zebrafish tissues (Oates et al., 2000; Wang et al., 2010; Zhao et al., 2001).

Over the past decade, the prokaryotic clustered regularly interspaced short palindromic repeats (CRISPR) and the CRISPR-associated system (Cas) (CRISPR/Cas system)-based technology has been successfully used in zebrafish to efficiently generate insertions and indels to disrupt gene function (Varshney et al., 2015). The Zon group designed a CRISPR-based vector system that enabled tissue-specific gene inactivation in zebrafish (Ablain et al., 2015). They later incorporated this system into the MiniCoopR (Ceol et al., 2011) vector and developed the CRISPR MiniCoopR vector for melanocyte-specific gene disruption and validated Spred1 loss as a driver of mucosal melanoma in zebrafish (Ablain et al., 2018). A similar approach has been used to disrupt the androgen receptor gene in zebrafish liver to determine its contribution in hepatocellular carcinoma (Li et al., 2019b). di Donato et al. (2016) used the Gal4-UAS system to control the expression of Cas9 and achieved tissue-specific gene disruption. The Chen group used different U6 promoters for multiplex single guide (sg)RNA expression and also demonstrated tissue-specific disruption (Yin et al., 2015). Our group incorporated the Zon and Chen methods into a gateway system to express multiple sgRNAs for gene disruption in neutrophils in zebrafish (Zhou et al., 2018). Although high efficiency is achieved, a major limitation is also observed: knockout efficiency reduces significantly when the knockout line is crossed with other fish lines that use neutrophil-specific promoters. This limitation created two

[1]Department of Biological Sciences, Purdue University, West Lafayette, IN 47907, USA. [2]Department of Molecular Genetics and Microbiology, and Immunology, Duke University School of Medicine, Durham, NC 27710, USA. [3]Department of Comparative Pathobiology, Purdue University, West Lafayette, IN 47907, USA. [4]Purdue Institute for Inflammation, Immunology, & Infectious Disease, Purdue University, West Lafayette, IN 47907, USA. [5]Purdue University Center for Cancer Research, Purdue University, West Lafayette, IN 47907, USA. [6]Purdue Institute for Integrative Neuroscience, Purdue University, West Lafayette, IN 47907, USA.
*Present address: Department of Lab Medicine, The Stem Cell Program, Boston Children's Hospital, Boston, MA 02115, USA; Department of Pathology, Harvard Medical School, Dana-Farber/Harvard Cancer Center, Boston, MA 02115, USA.
‡Present address: Joan and Sanford I. Weill Department of Medicine, Division of Gastroenterology, Weill Cornell Medicine, Cornell University, New York, NY 10065 USA.
§These authors contributed equally to this work

¶Author for correspondence (deng67@purdue.edu)

A.Y.H., 0000-0001-5680-345X; G.J.Z., 0000-0002-0839-5161; D.M.T., 0000-0003-3465-5518; Q.D., 0000-0002-9254-9951

Handling Editor: Daniel Billadeau
Received 24 February 2021; Accepted 1 March 2021

Journal of Cell Science (2021) 134, jcs258574. doi:10.1242/jcs.258574

problems: (1) without a sgRNA-resistant rescue construct, the specificity of the sgRNAs and the related phenotype cannot be concluded; and (2) incorporating biosensors into the knockout lines requires generating additional Cas9-2a-sensor lines, thereby limiting the flexibility of incorporating additional genetically encoded probes as projects evolve. We also found, to the best of our knowledge, that tissue-specific gene rescue and biosensor imaging in a tissue-specific knockout background have not yet been achieved in any previous work in zebrafish.

Here, we report an updated CRISPR/Cas9 system for a robust and flexible neutrophil-restricted knockout in zebrafish. We successfully disrupted different genes in neutrophils and applied live imaging using various biosensors in the knockout background. As a proof-of-principle, we inactivated the *rac2* gene. Rac2 is essential for actin polymerization, cell migration and intracellular signaling. Loss of Rac2 activity leads to defects in neutrophil motility and chemotaxis in zebrafish (Deng et al., 2011; Rosowski et al., 2016). However, it remains unknown whether Rac activation is restricted to the front of the cell during neutrophil migration *in vivo*. The specific functions of Rac2, in comparison to its homologue Rac1 that is also expressed in neutrophils, are also not clear. Using multiple biosensors, we observed that Rac activation and force bearing actin structures are localized to the cell front and back in zebrafish neutrophils in an oscillating fashion, and the localizations are dependent on Rac2. Together, our system here provides a robust tool for discovering and characterizing genes that regulate neutrophil migration *in vivo*.

RESULTS

A Gateway cloning system for a tissue-specific knockout

Our previous strategy was to express Cas9 tagged with mCherry specifically in neutrophils and the sgRNA ubiquitously to achieve a neutrophil-specific knockout (Zhou et al., 2018). We speculate that the presence of another construct driven by neutrophil-specific promoters in the genome may compete with the transcriptional factors for Cas9-2A-mCherry expression and reduces Cas9 protein to a level that is not sufficient for an efficient knockout. On the contrary, several studies incorporated the same tissue-specific promoter multiple times and still achieved sufficient target gene disruption using untagged Cas9 (Ablain et al., 2015; Ceol et al., 2011; Li et al., 2019b). Thus, we decided to use the untagged Cas9. We designed two different plasmids to express the Cas9 and sgRNA in two separate lines. To generate a final plasmid construct for cell-specific Cas9 expression, we used three entry plasmids, containing, respectively, the neutrophil-specific promoter lysozyme C (lyzC), Cas9 with nuclear localization sequences, SV40 polyA and a destination Tol2 vector with a GFP reporter gene driven by the *α-crystallin* (*cry*, also known as *cryaa*) promoter. GFP^{+} lenses enable the selection of zebrafish with stable genomic integration (Fig. 1A). To introduce ubiquitous sgRNA expression, we used a plasmid harboring a GFP reporter gene controlled by the *lyzC* promoter, and two gene-specific sgRNAs driven by the zebrafish RNA polymerase (RNAP) III-dependent U6 promoters (U6a and U6c) (Fig. 1B). The successful incorporation of sgRNA sequences into the zebrafish genome can be visualized by GFP expression in neutrophils.

To test the gene knockout efficiency, we injected the F2 embryos of the newly generated *Tg(lyzC:cas9, cry:GFP)*^{pu26} line with the plasmids carrying *rac2*-targeting sgRNAs or control (*ctrl*) sgRNAs for transient gene inactivation. The sequences of the sgRNAs are described in Fig. 1C,D. A longer sequence with no predicted binding sites in the zebrafish genome was used as a non-targeting control (Fig. 1D). As expected, we observed significantly decreased neutrophil motility in larvae of *Tg(lyzC:cas9, cry:GFP)*^{pu26} fish transiently expressing sgRNAs targeting *rac2* (Fig. 1E,F; Movie 1), consistent with a functional disruption of the *rac2* gene.

To test the knockout efficiency, we generated two transgenic lines, *Tg(U6a/*c: *ctrl sgRNAs, lyzC:GFP)*^{pu27} and *Tg(U6a/*c: *rac2 sgRNAs, lyzC:GFP)*^{pu28}. The F1 fish were crossed with

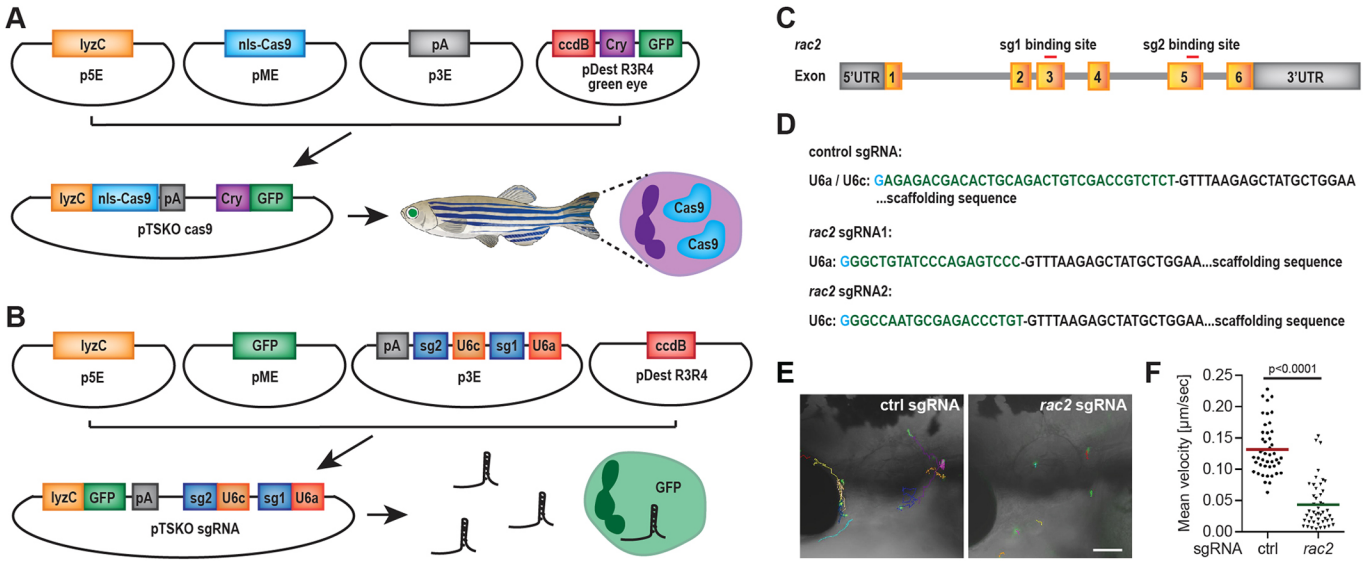

Fig. 1. Establishment of the neutrophil-specific knockout system. (A) Schematics of the gateway vectors to clone constructs for the zebrafish *Tg(LyzC:Cas9, Cry:GFP)*^{pu26} line with neutrophil-specific Cas9 expression and green lens. (B) Schematics of the gateway construct for ubiquitous expression of sgRNAs and neutrophil-specific expression of GFP or other reporters. (C) Schematic of the gene structure of the zebrafish *rac2* gene. The sgRNA1 and sgRNA2 target exon 3 and exon 5 in the forward strand, respectively. (D) Sequences of sgRNAs (control or *rac2* targeting). The first G (blue) is included in the backbone. (E,F) Representative images (E) and quantification (F) of neutrophil motility in the head mesenchyme of *Tg(LyzC:Cas9, Cry:GFP)*^{pu26} larvae injected with plasmids carrying control (ctrl) or *rac2* sgRNAs at 3 dpf. The individual points are mean speeds for individual neutrophils. The red and green lines indicate the mean velocity in each group. One representative result from three biological repeats is shown. n=45 for control, and n=46 for *rac2* transient knockouts from four different larvae. P<0.0001 (Mann–Whitney test). See also Movie 1. Scale bar: 100 µm.

Journal of Cell Science (2021) 134, jcs258574. doi:10.1242/jcs.258574

Tg(lyzC:cas9, cry:GFP)^{pu26}, and the velocity of neutrophils in the head mesenchyme was quantified in embryos at 3 days post fertilization (dpf). As expected, a significant decrease of motility was observed in the neutrophils expressing Cas9 protein and the *rac2* sgRNAs (Fig. 2A,B; Movie 2). To make sure that the sgRNA expression alone does not influence neutrophil motility, we compared neutrophil motility in the transgenic lines *Tg(U6a/c: ctrl sgRNAs, lyzC:GFP)*^{pu27} or *Tg(U6a/c: rac2 sgRNAs, lyzC:GFP)*^{pu28} with that in *Tg(lyzC:GFP)* (Hall et al., 2007). All lines displayed similar neutrophil motility, indicating that the migration defects are dependent on the expression of Cas9 in neutrophils (Fig. 2C,D; Movie 3). The *lyzC* is a well-characterized promoter for driving gene expression in neutrophils (Kitaguchi et al., 2009), albeit with a much lower expression level in macrophages. As Rac2 is also required for macrophage migration in tissue (Rosowski et al., 2016), we measured the speed of macrophage migration to infer the function of *rac2* in macrophages. To confirm that the Cas9-mediated depletion was neutrophil-specific, we bred in a macrophage reporter line *Tg(mpeg: mcherry-H2B)* (Davis et al., 2016) into the two lines described in Fig. 2A,B. Although neutrophil motility remained deficient (Fig. 2E,F), macrophage migration was intact (Fig. 2E,G; Movie 4), indicating that *rac2* inactivation in macrophages was not significant.

To demonstrate the editing of the *rac2* locus in neutrophils, we crossed *Tg(LyzC:Cas9, Cry:GFP)*^{pu26} with *Tg(U6a/c: ctrl sgRNAs, lyzC:GFP)*^{pu27} or *Tg(U6a/c: rac2 sgRNAs, LyzC:GFP)*^{pu28}, and the neutrophils from the 3 dpf larvae were enriched using fluorescence-activated cell sorting. The *rac2* sgRNA1 and sgRNA2 target sites were amplified and the PCR products were treated with T7 endonuclease 1 (T7E1). In neutrophils sorted from the *rac2* sgRNA expressing lines, sufficient genome editing was detected at the sgRNA1 targeting site, but not at the sgRNA2 targeting site (Fig. 2H). No editing was detected in the sorted neutrophils expressing control sgRNAs. To further demonstrate the specific gene disruption in neutrophils, we used a T7E1 assay to check the sgRNA target sites in the GFP^{-} non-neutrophil population. We did not observe significant editing (Fig. 2I), indicating that the *rac2* disruption is primarily restricted to neutrophils. We further deep sequenced these loci and detected a mutation efficiency of 34.73% at the sgRNA1 target site and 17.16% at the sgRNA2 target site (Fig. 2J), whereas in the GFP^{-} non-neutrophil population, a similar level of editing was not detected.

Expression of sgRNA-resistant *rac2* rescued the neutrophil migration defect

A gold standard to confirm that a particular phenotype results from a specific gene disruption is to perform a gene-specific rescue. We therefore replaced the GFP gene with a sgRNA-resistant *rac2* gene in the pME entry plasmid described in Fig. 1B and constructed the final plasmid to allow co-expression of the rescue gene and the sgRNAs (Fig. 3A). Restoring the expression of wild-type Rac2 rescued the neutrophil motility defect seen in embryos with neutrophil-specific *rac2* disruption (Fig. 3B,C; Movie 5), indicating that the motility

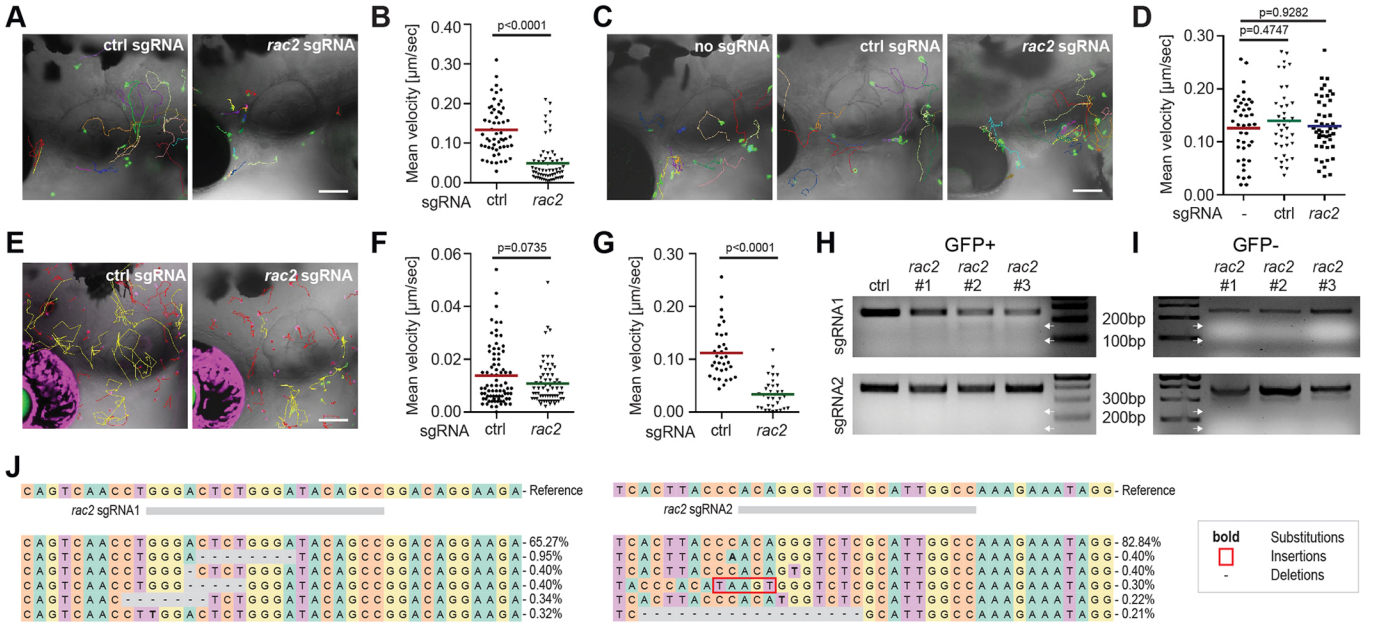

Fig. 2. Neutrophil-specific knockout of *rac2* in stable transgenic lines. Stable lines were generated by crossing *Tg(LyzC:Cas9, Cry:GFP)*^{pu26} with *Tg(U6a/c: ctrl guide, LyzC:GFP)*^{pu27} or *Tg(U6a/c: rac2 guides, LyzC:GFP)*^{pu28}. (A,B) Representative images (A) and quantification (B) of neutrophil motility in the head mesenchyme of 3 dpf larvae. *n*=55 for control from four different larvae and *n*=60 for *rac2* knockouts from five different larvae. *P*<0.0001 (Mann–Whitney test). (C,D) Representative images (C) and quantification (D) of neutrophil motility in the head mesenchyme of 3 dpf larvae. *n*=41 for *Tg(lyzC:GFP)*, *n*=38 for *Tg(u6a/c: ctrl sgRNA, lyzC:GFP)*^{pu27} and *n*=47 for *Tg(u6a/c: rac2 sgRNA, lyzC:GFP)*^{pu28} from three different larvae. *P*=0.9282 and *P*=0.4747 (one-way ANOVA). (E-G) *Tg(LyzC:Cas9, Cry:GFP)*^{pu26} was crossed with *Tg(U6a/c: ctrl guide, LyzC:GFP, mpeg:mcherry-H2B)* or *Tg(U6a/c: rac2 guides, LyzC:GFP, mpeg:mcherry-H2B)*. Representative images (E) and quantification of macrophage motility (F) and neutrophil motility (G) in the head mesenchyme of 3 dpf larvae. The macrophage tracks are red, and the neutrophil tracks are yellow. *n*=80 for macrophages in the control group and *n*=65 for macrophages in *rac2* knockouts. *n*=34 for neutrophils in the control group and *n*=32 for macrophages in *rac2* knockouts from four different larvae. *P*=0.0735 and *P*<0.0001 (Mann–Whitney test). In B,D,F and G, the individual points are mean speeds for individual cells. The red and green lines indicate the mean velocity in each group. (H,I) Adults from three separate founders in *Tg(LyzC:Cas9, Cry:GFP)*^{pu26} were crossed with *Tg(U6a/c: ctrl guide, LyzC:GFP)*^{pu27} or *Tg(U6a/c: rac2 guides, LyzC:GFP)*^{pu28}. Representative gel images of the T7E1-treated PCR products amplifying the sgRNA1 and sgRNA2 targeting sites from genomic DNA of sorted neutrophils (H) or non-neutrophil cells (I) from 3 dpf embryos. White arrows indicate the expected cleavage bands. (J) Deep sequencing of the *rac2* loci described in H. The sequences on the top are wild-type sequences, and the five most frequent types of mutations are shown. Point mutations, deletions and insertions are all observed. See also Movies 2, 3, 4. Scale bars: 100 µm.

Journal of Cell Science (2021) 134, jcs258574. doi:10.1242/jcs.258574

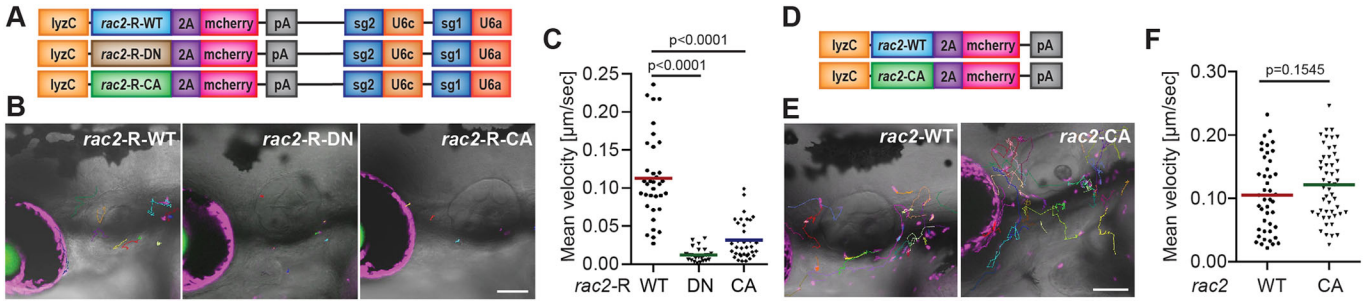

Fig. 3. Re-expression of *rac2* rescued neutrophil motility defects in neutrophil-specific *rac2* knockout fish. (A) Schematics of the plasmids for neutrophil-specific rescue. The sgRNA-resistant *rac2* gene of wild type (*rac2*-R-WT), dominant-negative (*rac2*-R-DN) or constitutively active (*rac2*-R-CA), along with the mCherry reporter gene, were cloned into the plasmid carrying *rac2* sgRNAs. (B,C) Representative tracks (B) and quantification (C) of neutrophil motility in the head mesenchyme of 3 dpf *Tg(lyzC:Cas9, cry:GFP)*^{pu26} larvae injected with plasmids encoding *rac2*-R (WT), *rac2*-R-*D57N* (DN) or *rac2*-R-*Q61L* (CA). *n*=35 for *rac2*-R-WT, *n*=27 for *rac2*-R-DN and *n*=35 for *rac2*-R-CA from four or five different larvae. *P*<0.0001 (one-way ANOVA). (D) Schematics of the plasmids used to generate stable *Tg(lyzC:rac2-2A-mcherry)*^{pu30} or *Tg(lyzC:rac2-Q61L-2A-mcherry)*^{pu29} lines. Representative tracks (E) and quantification (F) of neutrophil motility in the head mesenchyme of 3 dpf *Tg(lyzC:rac2-2A-mcherry)*^{pu30} or *Tg(lyzC: rac2-Q61L-2A-mcherry)*^{pu29} larvae. *n*=44 for *rac2*-WT and *n*=50 for *rac2*-CA from three different larvae. *P*=0.1545 (Mann–Whitney test). In C and F, the individual points are mean speeds for individual neutrophils. The red and green lines indicate the mean velocity in each group. See also Movies 5, 6. Scale bars: 100 µm.

defect is a result of the loss of Rac2 function in neutrophils. As controls, supplementing Rac2-deficient neutrophils with either a dominant-negative D57N (Deng et al., 2011), or a constitutively active Q61L version of RAC2 (Gu et al., 2001), failed to restore cell motility, indicating that spatially or temporally regulated Rac2 GTPase activity is required to drive neutrophil migration.

The RAC2 Q61L induces abnormal cell proliferation in human cells (Gu et al., 2001). However, whether this mutation impacts neutrophil migration is yet to be determined in both human and zebrafish. On this end, we generated a transgenic zebrafish line, *Tg(lyzC:mcherry-2A-Rac2CA)*^{pu29}, overexpressing the Rac2 Q61L in neutrophils (Fig. 3D). Interestingly, in the *Tg(lyzC:mcherry-2A-Rac2CA)*^{pu29} stable line, no significant change in neutrophil motility was observed compared to the *Tg(lyzC:mcherry-2A-Rac2WT)*^{pu30} line, which overexpresses wild-type Rac2 (Fig. 3E,F; Movie 6). Together, the Rac2 Q61L mutation does not have a dominant function but only impacts neutrophil mobility in the *rac2* knockout background.

Disruption of *cdk2* using the tissue-specific knockout system also suppressed neutrophil motility

Our previous study revealed an unexpected and critical role of Cdk2 in neutrophil migration and chemotaxis (Hsu et al., 2019). To ensure that the neutrophil-specific knockout system is feasible for disrupting other genes, we injected plasmids carrying *cdk2* targeting sgRNAs into *Tg(lyzC:cas9, cry:GFP)*^{pu26} embryos. Two sgRNAs targeting exon 4, which encodes the CDK2 catalytic domain were selected (Fig. 4A). Neutrophil motility was significantly reduced by the tissue-specific *cdk2* disruption (Fig. 4B,C; Movie 7), recapitulating the phenotypes observed in the stable lines overexpressing a kinase-dead dominant-negative form of Cdk2, D145N (DN) (Hsu et al., 2019). To confirm that neutrophil migration defects did indeed result from *cdk2* disruption, we again performed rescue experiments. Restoring wild type, but not the dominant-negative, Cdk2 expression partially rescued the neutrophil migration defects caused by *cdk2* gene disruption (Fig. 4D-F; Movie 8). Our results indicate that the Cdk2 kinase activity is required for neutrophil motility in zebrafish, and that the neutrophil-specific knockout system is a robust tool to reach this conclusion.

Neutrophil-specific *rac2* knockout disrupts Rac activation

To observe alternations of Rac activation resulting from *rac2* disruption, we used a Rac-binding domain of PAK1 fused with GFP (PBD-GFP) (Benink and Bement, 2005) to mark the location of active Rac in neutrophils. This reporter has been used in previous studies in human neutrophil-like HL-60 cells and revealed that active Rac localizes to the cell front during migration *in vitro* (Benard et al., 1999; Srinivasan et al., 2003; Peng et al., 2011). Again, we cloned

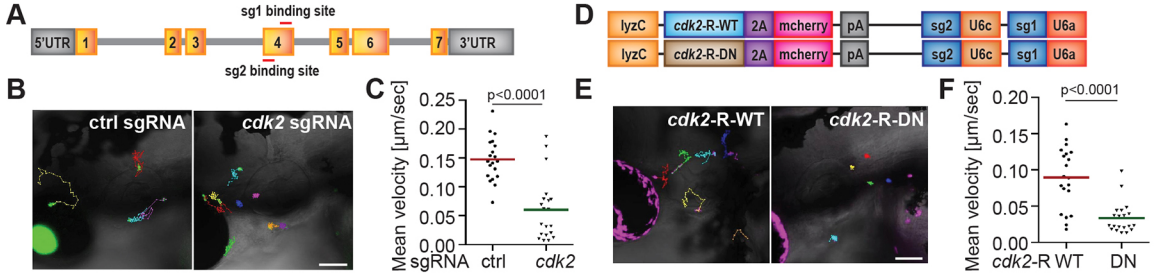

Fig. 4. Neutrophil-specific knockout of *cdk2* reduced neutrophil motility. (A) Schematic of the gene structure of the zebrafish *cdk2* gene. The two target sites of the sgRNAs are in exon 4. (B,C) Representative tracks (B) and quantification (C) of neutrophil motility in the head mesenchyme of 3 dpf *Tg(lyzC:Cas9, Cry:GFP)*^{pu26} larvae injected with plasmids carrying sgRNAs of control (ctrl) or *cdk2*. (D) Schematic diagrams of the plasmids used to rescue Cdk2 expression. (E,F) Representative tracks (E) and quantification (F) of neutrophil motility in the head mesenchyme of 3 dpf *Tg(lyzC:Cas9, Cry:GFP)*^{pu26} larvae injected with plasmids carrying *cdk2*-R-WT or *cdk2*-R-D145N (DN). *n*=20 for each group from three different larvae. *P*<0.0001 (Mann–Whitney test). In C and F, the individual points are mean speeds for individual neutrophils. The red and green lines indicate the mean velocity in each group. See also Movies 7, 8. Scale bars: 100 µm.

Journal of Cell Science (2021) 134, jcs258574. doi:10.1242/jcs.258574

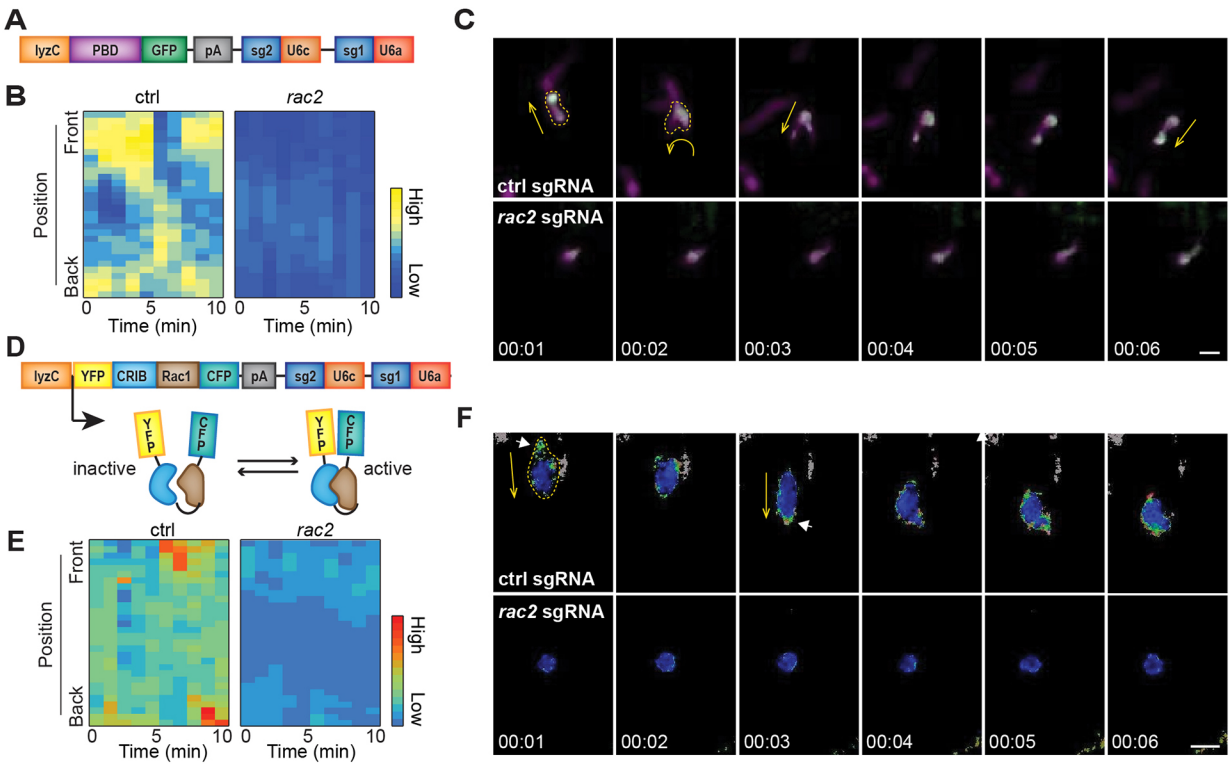

Fig. 5. Subcellular location of Rac activation in wild-type and *rac2*-deficient neutrophils. (A) Schematic diagram of the plasmid facilitating neutrophil-specific PBD-GFP expression and ubiquitous sgRNA expression. (B) Simultaneous imaging of PBD-GFP and cytosolic mCherry in neutrophils expressing either ctrl or *rac2* sgRNA. (C) Kymographs of PBD-GFP signal intensity along the axis of migration in neutrophils expressing either ctrl (upper) or *rac2* sgRNA (lower). (D) Schematic diagram of the plasmid, allowing neutrophil-specific Racihu-Rac1 expression and ubiquitous sgRNA expression. (E) Representative images of Rac activity in migrating neutrophils determined by ratiometric FRET live imaging. (F) Kymographs of Racihu-Rac1 FRET intensity along the axis of migration in neutrophils expressing either ctrl (upper) or *rac2* sgRNA (lower). In C and F, white arrows point to the location of active Rac and yellow arrows indicate the direction of cell migration. The yellow dashed lines outline cell borders. Data are representative of more than three separate time-lapse videos. See also Movies 9, 10. Scale bars: 10 µm.

this construct in the pME entry vector described in Fig. 1B and obtained the plasmid that allowed expression of the biosensor in the control or *rac2* knockout background (Fig. 5A). Here, in zebrafish, the PBD-GFP probe was enriched at both the front and rear in the migrating neutrophils in the control. When neutrophils migrate, Rac activity oscillated: active Rac first concentrated on the cell front and later shifted to the back. No discernible enrichment of Rac activity was detected in *rac2*-deficient neutrophils (Fig. 5B,C; Movie 9).

Forster resonance energy transfer (FRET)-based biosensors are used to detect protein conformational changes and interactions. To determine the subcellular location of Rac activation using a second approach, the 'Raichu' (Ras superfamily and interacting protein chimeric unit) Rac1-FRET probe developed by the Matsuda group (Itoh et al., 2002) was cloned into our sgRNA plasmids (Fig. 5D). When Rac is activated, the binding of Rac-GTP to PAK1-CRIB (CDC42/Rac interactive binding domain) increases FRET and the YFP/CFP fluorescence ratio. In neutrophils isolated from the 'Raichu' reporter mouse strain, active Rac localizes at both the front and back during chemotaxis (Johnsson et al., 2014). Consistent with this report, in zebrafish, Rac activity is higher at the cell periphery and oscillated between the front and back of migrating neutrophils expressing control sgRNAs. The *rac2*-defective neutrophils lost the ability to polarize and protrude, and did not display proper RAC activity (Fig. 5E,F; Movie 10), indicating that Rac2 function is required for the spatially and temporally coordinated Rac activation during neutrophil interstitial migration.

Neutrophil-specific *rac2* knockout alters actin cytoskeletal dynamics

To observe the alternations in the actin cytoskeleton resulting from *rac2* disruption, we used the calponin-homology domain of Utrophin (Utr-CH)-GFP (Burkel et al., 2007; Barros-Becker et al., 2017; Lam et al., 2014) to label stable F-actin in zebrafish neutrophils as described previously (Barros-Becker et al., 2017; Lam et al., 2014) (Fig. 6A). In *Tg(lyzC:cas9, cry:GFP)*^{pu26} larvae transiently expressing control sgRNAs, stable F-actin was enriched at the rear of migrating neutrophils. On the contrary, (Utr-CH)-GFP was not enriched at any specific subcellular locations in *rac2* knockout neutrophils (Fig. 6B,C; Movie 11), indicating a loss of stable actin and cell polarity.

An actin stress probe, actin–cpstFRET–actin (AcpA), was recently developed to report forces within F-actin filaments (Johnsson et al., 2014). The sensor consists of a FRET pair flanking two linked β-actin monomers. When incorporated into F-actin filaments, the mechanical force in the filaments twists AcpA and decreases FRET efficiency. Thus, actin stress can be inferred from CFP/YFP ratio (Fig. 6D). We expressed the sensor and control or *rac2* sgRNAs in *Tg(lyzC:cas9, cry:GFP)*^{pu26} embryos. Actin stress was relatively higher at the front and rear of neutrophils in control cells during migration. In contrast, *rac2* knockout neutrophils showed decreased actin stress (Fig. 6E,F; Movie 12), suggesting that Rac2 is required for actin polymerization and force generation. Taken together, the ease of incorporating various biosensors into the neutrophil-specific knockout system allows live imaging of dynamic signaling events during cell

Journal of Cell Science (2021) 134, jcs258574. doi:10.1242/jcs.258574

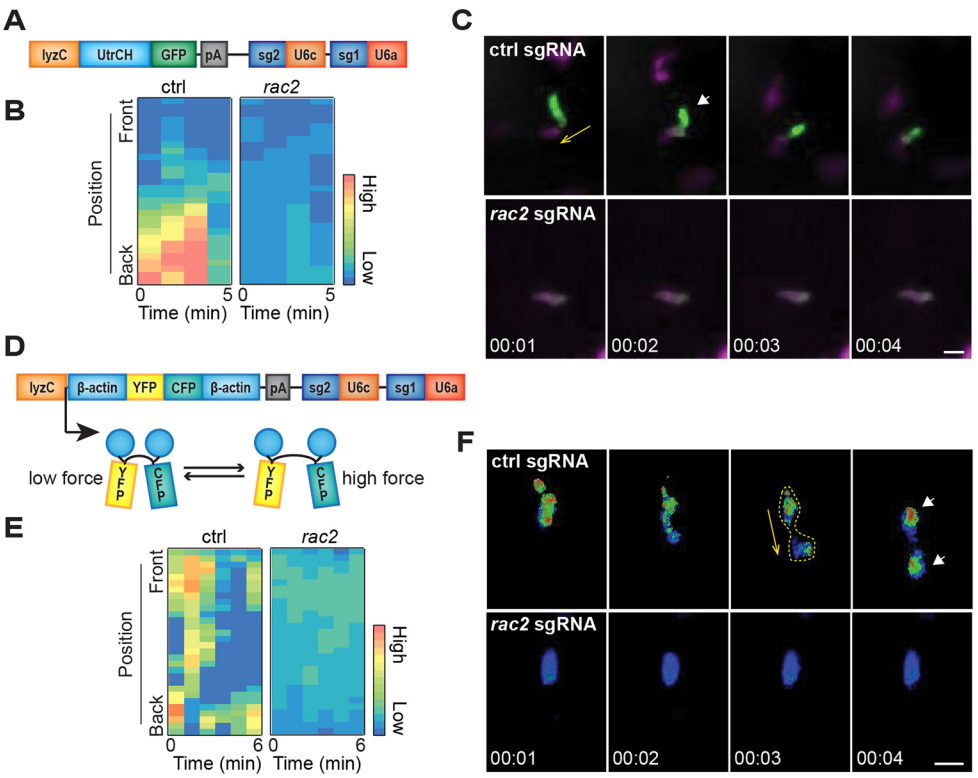

Fig. 6. Subcellular location of stable and stressed actin in wild-type and *rac2*-deficient neutrophils. (A) Schematic diagram of the plasmid facilitating neutrophil-specific Utr-CH-GFP expression and ubiquitous sgRNA expression. (B) Simultaneous imaging of UtrCH-GFP and cytosolic mCherry in neutrophils expressing either ctrl or *rac2* sgRNA. (C) Kymographs of Utr-CH-GFP intensity along the axis of migration in neutrophils expressing either ctrl sgRNA (upper) or *rac2* sgRNA (lower). (D) Schematic diagram of the plasmid facilitating neutrophil-specific AcpA-FRET expression and ubiquitous sgRNA expression. (E) Ratiometric FRET live imaging of AcpA-FRET in neutrophils expressing either ctrl sgRNA or *rac2* sgRNA. (F) Kymographs of AcpA-FRET intensity along the axis of migration in neutrophils expressing either ctrl sgRNA (upper) or *rac2* sgRNA (lower). In C and F, white arrows point to the location of stable actin or high actin stress, yellow arrows indicate the direction of cell migration. The yellow dashed lines outline cell borders. Data are representative of more than three separate time-lapse videos. See also Movies 11, 12. Scale bars: 10 µm.

migration in the knockout background, providing a flexible tool to interrogate gene function and determine mechanism.

Ribozyme-mediated gRNA generation for a neutrophil-specific knockout

We evaluated another gateway system for neutrophil-specific gene modification, in which the Cas9 protein is ubiquitously expressed and the sgRNA is processed by ribozymes and expressed in a neutrophil-restricted manner (Walton, 2018). This strategy was adapted from a previous study using an all-in-one plasmid containing a universal promoter (Lee et al., 2016). Here, we separated the Cas9 and sgRNA into two plasmids (Fig. 7A). The sgRNA is processed by the hammerhead and hepatitis delta virus ribozymes at the 5′ and 3′ ends, respectively. The noncoding RNA, MALAT1, forming a triple helical structure at the 3′ end (Wilusz et al., 2012), is incorporated to stabilize the tdTomato mRNA. The sgRNA and the tdTomato reporter gene is expressed as a single transcript driven by the lyzC promoter. We generated a transgenic zebrafish line, *Tg(ubb:cas9, cry:GFP)*^{xt48}, and cloned the same control and the *rac2* sgRNA1 into the ribozyme-mediated knockout system. The sgRNA plasmids carrying *rac2* sgRNA or *ctrl* sgRNA were injected into the F2 embryos of the *Tg(ubb:cas9, cry:GFP)*^{xt48} line. Neutrophil motility was significantly decreased in the zebrafish larvae carrying *rac2* sgRNA, indicating sufficient gene disruption (Fig. 7B,C; Movie 13). Notably, we observed a slight decrease in neutrophil motility when we transiently injected the control sgRNA plasmids into the wild-type background (Fig. 7D,E; Movie 14), raising some slight concerns regarding expressing the sgRNA using ribozyme-mediated processing machinery in neutrophils.

DISCUSSION

Here, we report a robust and flexible neutrophil-specific knockout system in zebrafish. Using the lens-restricted GFP expression, we can easily select the positive fish carrying the Cas9 transgene. Transient expression of sgRNAs and visualization of edited cells can be achieved by injecting plasmids containing sgRNAs and GFP into the Cas9-expressing embryos. We also demonstrated the knockout efficiency using sgRNAs targeting *rac2* and *cdk2* using neutrophil motility as a proxy. To establish a causal relationship between the phenotype and the sgRNA-mediated genome editing, we rescued the migration phenotype by expressing sgRNA-resistant *rac*2 or *cdk2*. The stable lines expressing Cas9 protein and *rac2* sgRNAs constructed here showed an inheritable ability to generate *rac2* knockout lines at the F2 generation. We expect that the Cas9-driver line can be maintained and crossed with different reporter lines with different sgRNAs to achieve a multiplexed knockout. With three lyzC promoter-driven constructs in one neutrophil, we were still able to observe the expected phenotypes (Fig. 5B, Fig. 6B).

The optimization of the CRISPR/Cas9 vectors from our previous research lies in: (1) removing the 2A-mcherry tag and (2) separating the Cas9 and sgRNA elements into two constructs. Although the knockout efficiency is acceptable with multiple genes in our previous system, gene-specific rescue or biosensor imaging in the knockout background was challenging. The updates described here overcome previous limitations and significantly increase the efficiency of making genetic changes in zebrafish, and understanding the resulting changes in cell structural and signaling molecules. An example of how this work changes our ability to probe mechanisms comes from our own previous experience. In 2017, we obtained a neutrophil-specific *mfn2* knockout line that displayed strong neutrophil adhesion defects. However, at that time, we encountered significant problems performing the rescue experiment or conducting a mechanistic study in the TSKO background. We could not observe mitochondrial morphology or related molecular/metabolic changes in any neutrophils with gene knockouts, and our work in zebrafish stopped with phenotypic observation. We only used zebrafish data for initial discovery, and the rest of the work was completed in human cells (Zhou et al., 2020). With the recent advance described here, we could have performed more

Journal of Cell Science (2021) 134, jcs258574. doi:10.1242/jcs.258574

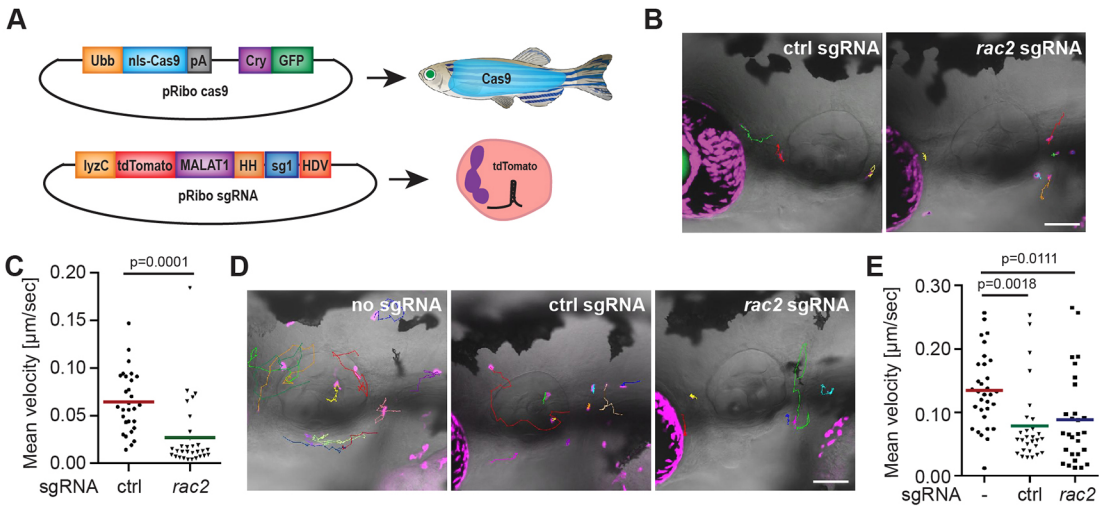

Fig. 7. Neutrophil-specific expression of ribozyme-processed *rac2*-targeting sgRNAs reduced neutrophil motility. (A) Schematic of the design of the plasmids for a second neutrophil-specific knockout system. Cas9 is expressed ubiquitously, whereas an sgRNA is expressed only in neutrophils. (B,C) Representative tracks (B) and quantification (C) of neutrophil motility in the head mesenchyme of 3 dpf *Tg(ubb:Cas9, cry:GFP)*^{xt48} larvae injected with plasmids carrying sgRNAs of control (ctrl) or *rac2*. *n*=29 for control and *n*=30 for *rac2* transient knockouts from three different larvae. *P*=0.0001 (Mann–Whitney test). (D,E) Representative tracks (D) and quantification (E) of neutrophil motility in the head mesenchyme of 3 dpf wild-type AB zebrafish larvae injected with Tol2-lyzC-RFP plasmid or plasmids carrying sgRNAs of control (ctrl) or *rac2*. *n*=32 for no sgRNA control from three different larvae, *n*=29 for control sgRNA and *n*=28 for *rac2* sgRNA from four different larvae. *P*=0.0018 and *P*=0.0111 (one-way ANOVA). In C and E, the individual points are mean speeds for individual neutrophils. The red and green lines indicate the mean velocity in each group. See also Movies 13, 14. Scale bars: 100 µm.

experiments in zebrafish and taken full advantage of this *in vivo* model for a mechanistic understanding of the genes of interest, such as *mfn2*.

As proof-of-principle, we applied our gateway cloning approach to study actin stress regulation in migrating neutrophils. It is known that the alignment of actin stress fibers in the cell body triggers cell polarization that precedes cell migration. However, actin networks and the actin stress distribution in living cells, especially in a three-dimensional tissue environment, are not well understood. Our work provides the first observation of the forces bared in actin filaments in migrating neutrophils *in vivo*. We observed higher mechanical force in actin at both the leading edge and the trailing edge. At the cell front, actin networks polymerize toward the direction of membrane protrusion and generate mechanical force to overcome membrane tension (Schaks et al., 2019; Sens and Plastino, 2015). The actin stress at the trailing edge is possibly related to actomyosin-mediated contraction, which facilitates the tail retraction (Wu et al., 2014). Our observations here contribute to the delineation of spatiotemporal actin stress regulation during three-dimensional migration of neutrophils (Hetmanski et al., 2019).

We also provide the first evidence that active Rac oscillates between the front and back of migrating neutrophils *in vivo*. Previously, the characterization of Rac activity localization was limited to *in vitro* studies on two-dimensional surfaces (Johnsson et al., 2014). The lamellipodium-based migration organized on monolayers on flat two-dimensional surfaces represents only one of many mechanisms of cell migration in three-dimensional environments in tissues (Petrie and Yamada, 2012, 2016). Owing to the distinct and interchangeable modes of migration and complex tissue environment, the subcellular location of Rac and its function during neutrophil migration at different sites *in vivo* was unclear. According to the prevalent local-excitation global-inhibition model in cell migration, the two processes, local excitation and global inhibition, are counter-regulatory. Upon stimulation, the rapid excitation response overcomes the slower inhibitory signals and initiates steep gradients in intracellular signaling, leading to cell polarization. Rac is considered one of the front-located proteins that amplify internal asymmetries that lead to further actin polarization induced by directional sensing signals (Franca-Koh and Devreotes, 2004; Kutscher et al., 2004). Using the PBD-GFP reporter for Rac, we show that the active Rac is enriched at the leading edge of the cell during protrusion, and shifts to the trailing edge during retraction. FRET imaging of Rac activity further confirmed this subcellular localization of Rac activation and indicates the potential involvement of Rac in tail contraction during neutrophil migration. Our observation of the subcellular location of active Rac in zebrafish neutrophils contributes to a better understanding of Rac signaling *in vivo*.

Notably, the Rac biosensors we used bind to both Rac1 and Rac2 proteins (Sells et al., 1997). Rac2 is the predominant isoform in human neutrophils (Heyworth et al., 1994). In murine neutrophils, the amounts of Rac1 and Rac2 are similar (Li et al., 2002), and Rac1 plays a major role in mediating tail retraction (Filippi et al., 2007). In zebrafish neutrophils, Rac2 is also the dominant isoform (Tell et al., 2012). We have previously used a transgene method to evaluate Rac function by expressing a dominant-negative form of Rac2 (Deng et al., 2011). The limitation of this approach is that dominant-negative Rac2 likely disrupted both Rac1 and Rac2 function. The overexpression of Rho family GTPases also raises the concern of the potential sequestration of GTPase regulating proteins, such as guanine-nucleotide-exchange factors (GEFs) and GTPase-activating proteins (GAPs). Here, using the tissue-specific knockout approach, we could dissect the biological function of Rac2 alone. It will be interesting and helpful to examine the unique functions and signaling pathways regulated by Rac1 and Rac2 in neutrophil migration in the future.

We also attempted using ribozymes to generate sgRNA in zebrafish neutrophils. Combined with the stable line expressing ubiquitous Cas9, this method also provides a viable approach for generating conditional mutants. An advantage of this system is that the same driver line, which drives ubiquitous Cas9 expression, can be used to knock out genes in different tissues. A previous report mentioned that sgRNA flanked by ribozymes are not fully

Journal of Cell Science (2021) 134, jcs258574. doi:10.1242/jcs.258574

processed in zebrafish (Lee et al., 2016). Our results indicate that this approach is efficient enough to induce a phenotype. However, we observed some reduction in cell speed when the ribozyme-flanking sgRNA was expressed alone. This effect could be tissue specific and will require careful evaluation in the future. Following this work, our aim is to expand functionality to allow multiplexed sgRNA expression. One direction to pursue is to evaluate both microRNA-based and tRNA-based processing machinery to process multiple sgRNAs from one transcript for tissue-specific gene disruption in zebrafish (Port and Bullock, 2016; Wang et al., 2015; Xie et al., 2015). The Cas12a family proteins have recently been demonstrated to mediate highly efficient genome editing in zebrafish, and will likely also enable tissue-specific disruption (Liu et al., 2019; Moreno-Mateos et al., 2017).

In summary, we developed a robust and flexible neutrophil-specific knockout system in zebrafish. Using this system, we gained insights into the role of Rac2 in regulating the actin cytoskeleton and the subcellular location of Rac activation in zebrafish neutrophils. Our system is suitable for various genetic studies and screens, which can be achieved by injecting plasmid encoding different sgRNAs into the Cas9-expression fish embryos. We also expect that our system can be adapted for gene function studies in various tissues using other tissue-specific promoters.

MATERIALS AND METHODS

Animals

The zebrafish experiment was conducted in accordance with internationally accepted standards. The Animal Care and Use Protocol was approved by the Purdue Animal Care and Use Committee, adhering to the Guidelines for Use of Zebrafish in the National Institutes of Health Intramural Research Program (protocol number 1401001018). MATLAB and the samplesizepwr function was used to calculate the sample sizes required for each experiment based on conservative estimates for the variability in the controls for each type of experiments, with a power of 0.9 (significance level of 0.05) in two sample *t*-test. Data were quantified blindly by an investigator not involved in data collection. To generate transgenic zebrafish lines, plasmids with the Tol2 backbone were co-injected with Tol2 transposase mRNA into embryos of the AB strain at the one-cell stage as described previously (Deng et al., 2011).

Plasmids

All plasmid constructs were generated by gateway cloning using LR Clonase II Plus enzyme (Invitrogen). The pME-Cas9 plasmid was obtained from Addgene (63154). The pME-GFP, p3E-polyA and the destination vector for the sgRNA plasmid, pDestTol2pA2, were obtained from the Tol2Kit (Kwan et al., 2007). To design sgRNAs, CRISPRscan (www.crisprscan.org/) was used. SgRNAs with the highest score and without any off-targets were selected. The destination vector pDestTol2pACryGFP (Addgene, 64022) was used to generate the final Cas9 plasmids. The p3E-U6a-U6c plasmids containing *rac2* sgRNAs or control sgRNAs (Addgene 107599, 107600), and p5E-lyzC (Addgene 107591) were described previously (Zhou et al., 2018).

In-Fusion cloning (In-Fusion HD Cloning Plus Kit, Clontech) was used to fuse the fragments with the linearized backbone, including the wild-type, dominant-negative or constitutively active guide-resistant *rac2* (ENSDARG00000038010), or different biosensor elements. The In-Fusion primers were as follows: pME-reverse remove GFP F, 5′-GCGGCCGCGGTGGAGCTCCAG-3′; pME-reverse remove GFP R, 5′-GGTGGCGAGTCGACCTCGAGGGG-3′; Rac-WT-guide1muta-pME F, 5′-TCTAGGCCTATGGGACACCGCAGGCCAAGAAGATTATGACAGACTGCGGCC-3′; Rac-WT-guide1muta-pME R, 5′-TCCCATAGGCCTAGATTTACCGGCTTGCTATCCACCATTACATTTGCAGAG-3′; Rac-DN-guide1muta-pME-F, 5′-TAGGCCTATGGAACACCGCAGGCCAAGAAGATTATGACAGACTGCGGCC-3′; Rac-DN-guide1muta-pME-R, 5′-TGTTCCATAGGCCTAGATTTACCGGTTTGCTATCCACCATTACATTTGC-3′; Rac-CA-guide1muta-pME-F, 5′-TCTAGGCCTATGGGACACCGCAGGCCTGGAAGATTATGACAGACTGCGG-3′; Rac-CA-guide1muta-pME-R, 5′-TCCCATAGGCCTAGATTTACCGGTTTGCTATCCACCATTACATTTGC-3′; Rac-guide2-resistant mutant F, 5′-GCAAGGACTTGCCTTAGCAAAGGAAATAGATGCAGTAAAATACCTGG-3′; Rac-guide2-resistant mutant R, 5′-AAGGCAAGTCCTTGCGGATAAGTGATCGGTGCCAGTTTC-3′; Rac-resistant into pME F, 5′-CGGGCCCCCCCTCGAGGCCACCATGGTGAGCAAGG-3′; Rac-resistant into pME R, 5′-AGCTCCACCGCGGCCGCTTAGAGCATCACGCAGCCC-3′, Rac-rescue-pME-F, 5′-GGTCGACTCGCCACCATGGTGAGCAAGGGCGAGG-3′, Rac-rescue-pME-R, 5′-CTCCACCGCGGCCGCTTAGAGCATCACGCAGCCC-3′; Rac-pME-R, 5′-AGCTCCACCGCGGCCGCTTAGAGCATCACGCAGCCC-3′; Cdk2-guide-1 F, 5′-AAGCCTCAAAACCTGCTGATCAACGCTCAGGGCGAGATC-3′; Cdk2-guide-1 R, 5′-CAGCAGGTTTTGAGGCTTAAGATCTCTGTGAAGAACCCG-3′; Cdk2-guide-1 mutant, 5′-cgggttcttcacagagatcttAAGCCTCAAAACCTGCTG-3′; Cdk2-guide-2 F, 5′-TACACCCACGAAGTTgtaactttgtggtacagagctcc-3′; Cdk2-guide-2 R, 5′-AACTTCGTGGGTGTAagtccgcacaggtacaccgaacgc-3′; Cdk2-guide-2 mutant, 5′-gcgttcggtgtacctgtgcggactTACACCCACGAAGTT-3′; ActinFRET-F-pME, 5′-GGTCGACTCGCCACCATGGATGATGATATCGCCGCGC-3′; ActinFRET-R-pME, 5′-CTCCACCGCGGCCGCCACCGCGGCCGCTTTAGAAG-3′; Utrophin-pME F, 5′-GGTCGACTCGCCACCATGGCCAAGTATGGAGAACATGAAG-3′; Utrophin-pME R, 5′-CTCCACCGCGGCCGCTTACTTGTACAGCTCGTCCATGCC-3′; PBD-F-pME, 5′-GGTCGACTCGCCACCAATACAAGCTACTTGTTCTTTTTGC-3′; PBD-R-pME, 5′-CTCCACCGCGGCCGCCTACGTAATACGACTCACTATAG-3′; RacFRET-F-pME, 5′-GGTCGACTCGCCACCATGGTGAGCAAGGGCGAGG-3′; RacFRET-R-pME, 5′-CTCCACCGCGGCCGCTTACATAATTACACACTTTGTC-3′; To clone sgRNAs for Ribozyme procession, the following primers were used: Ribo Ctrl F, 5′-GTATTGGTCTGCGAGAGACTGCTGATGAGTCCGTGAGGACGAAACGAGTAAGCTCGTC-3′; Ribo Ctrl R, 5′-ACTTGCTATTTCTAGCTCTAAAACGAGACGACACTGCAGACTGGACGAGCTTACTCGTT-3′-; Ribo Rac guide F, 5′-GTATTGGTCTGCGAGCACTCCCTGATGAGTCCGTGAGGACGAAACGAGTAAGCTCGTC-3′; and Ribo Rac guide R, 5′-ACTTGCTATTTCTAGCTCTAAAACCAGACGGTAAACACCACTCCGACGAGCTTACTCGTT-3′. To generate pME and p3E ribozyme sgRNAs, the empty pME-RZsgRNA and/or empty p3E-RZsgRNA was digested with AatII. Primers designed using the Oligo Design tool (Table S1) were annealed and extended using a standard PCR reaction then inserted into the digested backbone using In-Fusion cloning.

Microinjection

Microinjections were performed as described previously (Deng et al., 2011). We injected 1 nl of a mixture containing 25 ng/µl plasmids and 35 ng/µl Tol2 transposase mRNA dissolved in an isotonic solution into the cytoplasm of embryos at the one-cell stage. The stable lines were generated as described previously (Deng et al., 2011). At least two founders (F0) for each line were obtained. Experiments were performed with F2 larvae produced by F1 fish derived from multiple founders. For transient knockout, only plasmids were injected into the *Tg(lyzC:cas9, cry:GFP)*^{pu26} transgenic line.

Live imaging

Larvae at 3 dpf were placed on a glass-bottom dish, and imaging was performed at 28°C. Time-lapse fluorescence images for neutrophil motility were obtained using a laser scanning confocal microscope (Zeiss LSM 710) with a 20× objective at 1-min intervals for 30 min. The green and red channels were acquired sequentially with 0.3-3% power of the lasers. Neutrophil migration with the expression of biosensors was captured every 1 min for 10 min. To track macrophage behavior together with neutrophils, larvae were mounted in glass-bottom dishes as described previously (Barros-Becker et al., 2017), and images were captured every 3 min for 2.5 h. For (Utr-CH)-GFP and PBD-GFP, the green and red channels were acquired with 0.3-5% power of the 488-nm laser and 0.5-2% power of the 561-nm laser, respectively. The 458-nm laser channel with 75% power was used for the AcpA-FRET and Rac-FRET biosensors. The fluorescent stacks were flattened using the maximum intensity projection and overlaid with or without a single slice of the bright-field image. All imaging procedures were

performed at temperatures between 26 and 28°C. The cell velocity was quantified using ImageJ with the MTrackJ plug-in and plotted in Prism 6.0 (GraphPad). The fluorescence intensity quantification was performed using an algorism written in our lab (https://github.com/tomato990/subcellular-intensity-reader). The kymograph was generated using Helm 1.0 (Deng et al., 2014).

T7 endonuclease I assay

T7 endonuclease I (New England Biolabs, M0302) was used to detect mutations caused by CRISPR/Cas9. Neutrophils and non-neutrophil cells were sorted based on GFP expression as described previously (Hsu et al., 2019). Genomic DNA containing sgRNA recognition sites was amplified by PCR from sorted cells. PCR products were purified with a PCR purification kit (Clontech) and re-annealed in a thermocycler using the following conditions: 95°C for 5 min; 95-85°C with a ramp rate of −0.3°C/s; and 85-25°C with a ramp rate of −0.1°C/s. Re-annealed PCR products were incubated with T7 endonuclease I at 37°C for 1 h, followed by agarose gel electrophoresis. Primers used for this assay are described below.

Mutational efficiency quantification

To determine the mutation efficiency in *Tg(LyzC:Cas9, Cry:GFP, U6a/c:rac2 guides, LyzC:GFP)*, the *rac2* loci around the sgRNA binding site was amplified by PCR using the following primers: Rac2-sgRNA1-F, 5′-GTGAGTATCACATCAGTAAGAG-3′; Rac2-sgRNA1-R, 5′-GTCCAGCTGAATGTCTGTAGTG-3′; Rac2-sgRNA2-F, 5′-GGCTGTATCTAGTCAAGAGATAG-3′; and Rac2-sgRNA2-R, 5′-GCATCATTGTTGCATGACAAC-3′. Amplification was followed by wide sequencing at the sequencing center at Purdue University. Mutational efficiency was calculated using the CRISPResso2 package (Clement et al., 2019; www.github.com/pinellolab/CRISPResso2).

Statistical analysis

Statistical analysis was performed using Prism 6 (GraphPad). An unpaired two-tailed Student's *t*-test or one-way ANOVA were used to determine the statistical significance of differences between groups. $P<0.05$ was considered statistically significant. Individual P values are indicated in the figures, with no data points excluded from statistical analysis. One representative experiment of at least three independent repeats is shown.

Acknowledgements

We thank Dr David Umulis (Purdue University) for critical reading of our manuscript and insightful comments. Raichu-Rac1 was a generous gift from Dr Miki Matsuda (Kyoto University, Japan).

Competing interests

The authors declare no competing or financial interests.

Author contributions

Conceptualization: Y.W., E.M.W., G.Z., D.M.T., Q.D.; Methodology: Y.W., A.Y.H., E.M.W., G.Z., D.M.T., Q.D.; Software: Y.W.; Validation: Y.W., A.Y.H., C.D., A.P.L.; Formal analysis: Y.W., A.Y.H.; Investigation: Y.W., A.Y.H., E.M.W., S.J.P., R.S., T.W., W.Z., C.D., A.P.L.; Resources: Y.W., A.Y.H., E.M.W., T.W., W.Z., D.M.T.; Data curation: Y.W., A.Y.H., R.S., C.D., A.P.L.; Writing - original draft: Y.W., Q.D.; Writing - review & editing: Y.W., G.Z., D.M.T., Q.D.; Visualization: Y.W., A.Y.H.; Supervision: Q.D.; Project administration: G.Z., D.M.T., Q.D.; Funding acquisition: G.Z., D.M.T., Q.D.

Funding

This work was supported by the National Institutes of Health (R35GM119787 to D.Q.; AI125517, AI130236 and AI127115 to D.T.; and R35GM124913 to G.Z.); and the Purdue Center for Cancer Research (P30CA023168, for shared resources). A.Y.H. was supported by a Cagiantas Fellowship, Purdue University. Deposited in PMC for release after 12 months.

Data availability

Raw sequencing reads have been deposited to the NCBI Sequence Read Archive under BioProject accession PRJNA706779

References

Ablain, J., Durand, E. M., Yang, S., Zhou, Y. and Zon, L. I. (2015). A CRISPR/Cas9 vector system for tissue-specific gene disruption in zebrafish. *Dev. Cell* **32**, 756-764. doi:10.1016/j.devcel.2015.01.032

Ablain, J., Xu, M., Rothschild, H., Jordan, R. C., Mito, J. K., Daniels, B. H., Bell, C. F., Joseph, N. M., Wu, H., Bastian, B. C. et al. (2018). Human tumor genomics and zebrafish modeling identify SPRED1 loss as a driver of mucosal melanoma. *Science* **362**, 1055-1060. doi:10.1126/science.aau6509

Barros-Becker, F., Lam, P. Y., Fisher, R. and Huttenlocher, A. (2017). Live imaging reveals distinct modes of neutrophil and macrophage migration within interstitial tissues. *J. Cell Sci.* **130**, 3801-3808. doi:10.1242/jcs.206128

Benard, V., Bohl, B. P. and Bokoch, G. M. (1999). Characterization of Rac and Cdc42 activation in chemoattractant- stimulated human neutrophils using a novel assay for active GTPases. *J. Biol. Chem.* **274**, 13198-13204. doi:10.1074/jbc.274.19.13198

Benink, H. A. and Bement, W. M. (2005). Concentric zones of active RhoA and Cdc42 around single cell wounds. *J. Cell Biol.* **168**, 429-439. doi:10.1083/jcb.200411109

Branda, C. S. and Dymecki, S. M. (2004). Talking about a revolution: The impact of site-specific recombinases on genetic analyses in mice. *Dev. Cell* **6**, 7-28. doi:10.1016/S1534-5807(03)00399-X

Burkel, B. M., von Dassow, G. and Bement, W. M. (2007). Versatile fluorescent probes for actin filaments based on the actin-binding domain of utrophin. *Cell Motil. Cytoskelet.* **64**, 822-832. doi:10.1002/cm.20226

Cantù, C., Felker, A., Zimmerli, D., Prummel, K. D., Cabello, E. M., Chiavacci, E., Méndez-Acevedo, K. M., Kirchgeorg, L., Burger, S., Ripoll, J. et al. (2018). Mutations in Bcl9 and Pygo genes cause congenital heart defects by tissue-specific perturbation of Wnt/β-catenin signaling. *Genes Dev.* **32**, 1443-1458. doi:10.1101/gad.315531.118

Ceol, C. J., Houvras, Y., Jane-Valbuena, J., Bilodeau, S., Orlando, D. A., Battisti, V., Fritsch, L., Lin, W. M., Hollmann, T. J., Ferré, F. et al. (2011). The histone methyltransferase SETDB1 is recurrently amplified in melanoma and accelerates its onset. *Nature* **471**, 513-518. doi:10.1038/nature09806

Clement, K., Rees, H., Canver, M. C., Gehrke, J. M., Farouni, R., Hsu, J. Y., Cole, M. A., Liu, D. R., Joung, J. K., Bauer, D. E. et al. (2019). CRISPResso2 provides accurate and rapid genome editing sequence analysis. *Nat. Biotechnol.* **37**, 224-226. doi:10.1038/s41587-019-0032-3

Davis, J. M., Huang, M., Botts, M. R., Hull, C. M. and Huttenlocher, A. (2016). A zebrafish model of cryptococcal infection reveals roles for macrophages, endothelial cells, and neutrophils in the establishment and control of sustained fungemia. *Infect. Immun.* **84**, 3047-3062. doi:10.1128/IAI.00506-16

Deng, Q. and Huttenlocher, A. (2012). Leukocyte migration from a fish eye's view. *J. Cell Sci.* **125**, 3949-3956. doi:10.1242/jcs.093633

Deng, Q., Yoo, S. K., Cavnar, P. J., Green, J. M. and Huttenlocher, A. (2011). Dual roles for Rac2 in neutrophil motility and active retention in Zebrafish hematopoietic tissue. *Dev. Cell* **21**, 735-745. doi:10.1016/j.devcel.2011.07.013

Deng, W., Wang, Y., Liu, Z., Cheng, H. and Xue, Y. (2014). HemI: a toolkit for illustrating heatmaps. *PLoS ONE* **9**, e111988. doi:10.1371/journal.pone.0111988

de Rienzo, G., Gutzman, J. H. and Sive, H. (2012). Efficient shRNA-mediated inhibition of gene expression in Zebrafish. *Zebrafish* **9**, 97-107. doi:10.1089/zeb.2012.0770

di Donato, V., de Santis, F., Auer, T. O., Testa, N., Sánchez-Iranzo, H., Mercader, N., Concordet, J.-P. and del Bene, F. (2016). 2C-Cas9: a versatile tool for clonal analysis of gene function. *Genome Res.* **26**, 681-692. doi:10.1101/gr.196170.115

Dong, J. and Stuart, G. W. (2004). Transgene manipulation in zebrafish by using recombinases. *Methods Cell Biol.* **2004**, 363-379. doi:10.1016/S0091-679X(04)77020-X

Dong, M., Fu, Y.-F., Du, T.-T., Jing, C.-B., Fu, C.-T., Chen, Y., Jin, Y., Deng, M. and Liu, T. X. (2009). Heritable and Lineage-Specific Gene Knockdown in Zebrafish Embryo. *PLoS ONE* **4**, e6125. doi:10.1371/journal.pone.0006125

Driever, W., Stemple, D., Schier, A. and Solnica-Krezel, L. (1994). Zebrafish: genetic tools for studying vertebrate development. *Trends Genet.* **10**, 152-159. doi:10.1016/0168-9525(94)90091-4

Filippi, M.-D., Szczur, K., Harris, C. E. and Berclaz, P. Y. (2007). Rho GTPase Rac1 is critical for neutrophil migration into the lung. *Blood* **109**, 1257-1264. doi:10.1182/blood-2006-04-017731

Franca-Koh, J. and Devreotes, P. N. (2004). Moving forward: mechanisms of chemoattractant gradient sensing. *Physiology* **19**, 300-308. doi:10.1152/physiol.00017.2004

Gu, Y., Jia, B., Yang, F.-C., D'Souza, M., Harris, C. E., Derrow, C. W., Zheng, Y. and Williams, D. A. (2001). Biochemical and biological characterization of a human Rac2 GTPase mutant associated with phagocytic immunodeficiency. *J. Biol. Chem.* **276**, 15929-15938. doi:10.1074/jbc.M010445200

Hall, C., Flores, M., Storm, T., Crosier, K. and Crosier, P. (2007). The zebrafish lysozyme C promoter drives myeloid-specific expression in transgenic fish. *BMC Dev. Biol.* **7**, 42. doi:10.1186/1471-213X-7-42

Hans, S., Kaslin, J., Freudenreich, D. and Brand, M. (2009). Temporally-controlled site-specific recombination in Zebrafish. *PLoS ONE* **4**, e4640. doi:10.1371/journal.pone.0004640

Hetmanski, J. H. R., de Belly, H., Busnelli, I., Waring, T., Nair, R. V., Sokleva, V., Dobre, O., Cameron, A., Gauthier, N., Lamaze, C. et al. (2019). Membrane tension orchestrates rear retraction in matrix-directed cell migration. *Dev. Cell* **51**, 460-475.e10. doi:10.1016/j.devcel.2019.09.006

Heyworth, P. G., Bohl, B. P., Bokoch, G. M. and Curnutte, J. T. (1994). Rac translocates independently of the neutrophil NADPH oxidase components p47(phox) and p67(phox). Evidence for its interaction with flavocytochrome b558. *J. Biol. Chem.* **269**, 30749-30752. doi:10.1016/S0021-9258(18)47341-3

Hoess, R. H. and Abremski, K. (1985). Mechanism of strand cleavage and exchange in the Cre-lox site-specific recombination system. *J. Mol. Biol.* **181**, 351-362. doi:10.1016/0022-2836(85)90224-4

Hsu, A. Y., Wang, D., Liu, S., Lu, J., Syahirah, R., Bennin, D. A., Huttenlocher, A., Umulis, D. M., Wan, J. and Denga, Q. (2019). Phenotypical microRNA screen reveals a noncanonical role of CDK2 in regulating neutrophil migration. *Proc. Natl. Acad. Sci. USA* **116**, 18561-18570. doi:10.1073/pnas.1905221116

Itoh, R. E., Kurokawa, K., Ohba, Y., Yoshizaki, H., Mochizuki, N. and Matsuda, M. (2002). Activation of Rac and Cdc42 video imaged by fluorescent resonance energy transfer-based single-molecule probes in the membrane of living cells. *Mol. Cell. Biol.* **22**, 6582-6591. doi:10.1128/MCB.22.18.6582-6591.2002

Johnsson, A.-K. E., Dai, Y., Nobis, M., Baker, M. J., McGhee, E. J., Walker, S., Schwarz, J. P., Kadir, S., Morton, J. P., Myant, K. B. et al. (2014). The Rac-FRET mouse reveals tight spatiotemporal control of Rac activity in primary cells and tissues. *Cell Reports* **6**, 1153-1164. doi:10.1016/j.celrep.2014.02.024

Kelly, A. and Hurlstone, A. F. (2011). The use of RNAi technologies for gene knockdown in zebrafish. *Brief. Funct. Genomics* **10**, 189-196. doi:10.1093/bfgp/elr014

Kitaguchi, T., Kawakami, K. and Kawahara, A. (2009). Transcriptional regulation of a myeloid-lineage specific gene lysozyme C during zebrafish myelopoiesis. *Mech. Dev.* **126**, 314-323. doi:10.1016/j.mod.2009.02.007

Kutscher, B., Devreotes, P. and Iglesias, P. A. (2004). Local excitation, global inhibition mechanism for gradient sensing: an interactive applet. *Science's STKE* **2004**, pl3. doi:10.1126/stke.2192004pl3

Kwan, K. M., Fujimoto, E., Grabher, C., Mangum, B. D., Hardy, M. E., Campbell, D. S., Parant, J. M., Yost, H. J., Kanki, J. P. and Chien, C.-B. (2007). The Tol2kit: a multisite gateway-based construction Kit for Tol2 transposon transgenesis constructs. *Dev. Dyn.* **236**, 3088-3099. doi:10.1002/dvdy.21343

Lam, P.-Y., Fischer, R. S., Shin, W. D., Waterman, C. M. and Huttenlocher, A. (2014). Spinning disk confocal imaging of neutrophil migration in Zebrafish. *Methods Mol. Biol.* **1124**, 219-233. doi:10.1007/978-1-62703-845-4_14

Langenau, D. M., Feng, H., Berghmans, S., Kanki, J. P., Kutok, J. L. and Look, A. T. (2005). Cre/lox-regulated transgenic zebrafish model with conditional myc-induced T cell acute lymphoblastic leukemia. *Proc. Natl. Acad. Sci. USA* **102**, 6068-6073. doi:10.1073/pnas.0408708102

Lawson, N. D. and Wolfe, S. A. (2011). Forward and reverse genetic approaches for the analysis of vertebrate development in the Zebrafish. *Dev. Cell* **21**, 48-64. doi:10.1016/j.devcel.2011.06.007

Lee, R. T. H., Ng, A. S. M. and Ingham, P. W. (2016). Ribozyme mediated gRNA Generation for in vitro and in vivo CRISPR/Cas9 mutagenesis. *PLoS ONE* **11**, e0166020. doi:10.1371/journal.pone.0166020

Li, S., Yamauchi, A., Marchal, C. C., Molitoris, J. K., Quilliam, L. A. and Dinauer, M. C. (2002). Chemoattractant-Stimulated Rac activation in wild-type and Rac2-deficient murine neutrophils: preferential activation of Rac2 and Rac2 gene dosage effect on neutrophil functions. *J. Immunol.* **169**, 5043-5051. doi:10.4049/jimmunol.169.9.5043

Li, W., Zhang, Y., Han, B., Li, L., Li, M., Lu, X., Chen, C., Lu, M., Zhang, Y., Jia, X. et al. (2019a). One-step efficient generation of dual-function conditional knockout and geno-tagging alleles in zebrafish. *eLife* **8**, e48081.

Li, H., Li, Y., Lu, J. W., Huo, X. and Gong, Z. (2019b). Liver-specific androgen receptor knockout attenuates early liver tumor development in zebrafish. *Sci. Rep.* **9**, 10645. doi:10.1038/s41598-019-46378-3

Lieschke, G. J. and Trede, N. S. (2009). Fish immunology. *Curr. Biol.* **19**, 678-682. doi:10.1016/j.cub.2009.06.068

Liu, P., Luk, K., Shin, M., Idrizi, F., Kwok, S., Roscoe, B., Mintzer, E., Suresh, S., Morrison, K., Frazão, J. B. et al. (2019). Enhanced Cas12a editing in mammalian cells and zebrafish. *Nucleic Acids Res.* **47**, 4169-4180. doi:10.1093/nar/gkz184

Moreno-Mateos, M. A., Fernandez, J. P., Rouet, R., Vejnar, C. E., Lane, M. A., Mis, E., Khokha, M. K., Doudna, J. A. and Giraldez, A. J. (2017). CRISPR-Cpf1 mediates efficient homology-directed repair and temperature-controlled genome editing. *Nat. Commun.* **8**, 2024. doi:10.1038/s41467-017-01836-2

Oates, A. C., Bruce, A. E. E. and Ho, R. K. (2000). Too much interference: injection of double-stranded RNA has nonspecific effects in the zebrafish embryo. *Dev. Biol.* **224**, 20-28. doi:10.1006/dbio.2000.9761

Pan, X., Wan, H., Chia, W., Tong, Y. and Gong, Z. (2005). Demonstration of site-directed recombination in transgenic zebrafish using the Cre/loxP system. *Transgenic Res.* **14**, 217-223. doi:10.1007/s11248-004-5790-z

Peng, G. E., Wilson, S. R. and Weiner, O. D. (2011). A pharmacological cocktail for arresting actin dynamics in living cells. *Mol. Biol. Cell* **22**, 3986-3994. doi:10.1091/mbc.e11-04-0379

Petrie, R. J. and Yamada, K. M. (2012). At the leading edge of three-dimensional cell migration. *J. Cell Sci.* **125**, 5917-5926. doi:10.1242/jcs.093732

Petrie, R. J. and Yamada, K. M. (2016). Multiple mechanisms of 3D migration: the origins of plasticity. *Curr. Opin. Cell Biol.* **42**, 7-12. doi:10.1016/j.ceb.2016.03.025

Port, F. and Bullock, S. L. (2016). Augmenting CRISPR applications in Drosophila with tRNA-flanked sgRNAs. *Nat. Methods* **13**, 852-854. doi:10.1038/nmeth.3972

Rosowski, E. E., Deng, Q., Keller, N. P. and Huttenlocher, A. (2016). Rac2 Functions in both neutrophils and macrophages to mediate motility and host defense in larval Zebrafish. *J. Immunol.* **197**, 4780-4790. doi:10.4049/jimmunol.1600928

Schaks, M., Giannone, G. and Rottner, K. (2019). Actin dynamics in cell migration. *Essays Biochem.* **63**, 483-495. doi:10.1042/EBC20190015

Sells, M. A., Knaus, U. G., Bagrodia, S., Ambrose, D. M., Bokoch, G. M. and Chernoff, J. (1997). Human p21-activated kinase (Pak1) regulates actin organization in mammalian cells. *Curr. Biol.* **7**, 202-210. doi:10.1016/S0960-9822(97)70091-5

Sens, P. and Plastino, J. (2015). Membrane tension and cytoskeleton organization in cell motility. *J. Phys. Condens. Matter* **27**, 273103. doi:10.1088/0953-8984/27/27/273103

Srinivasan, S., Wang, F., Glavas, S., Ott, A., Hofmann, F., Aktories, K., Kalman, D. and Bourne, H. R. (2003). Rac and Cdc42 play distinct roles in regulating PI(3,4,5)P3 and polarity during neutrophil chemotaxis. *J. Cell Biol.* **160**, 375-385. doi:10.1083/jcb.200208179

Tell, R. M., Kimura, K. and Palić, D. (2012). Rac2 expression and its role in neutrophil functions of zebrafish (Danio rerio). *Fish Shellfish Immunol.* **33**, 1086-1094. doi:10.1016/j.fsi.2012.07.020

Thummel, R., Burket, C. T., Brewer, J. L., Sarras, M. P., Li, L., Perry, M., McDermott, J. P., Sauer, B., Hyde, D. R. and Godwin, A. R. (2005). Cre-mediated site-specific recombination in zebrafish embryos. *Dev. Dyn.* **233**, 1366-1377. doi:10.1002/dvdy.20475

Varshney, G. K., Pei, W., Lafave, M. C., Idol, J., Xu, L., Gallardo, V., Carrington, B., Bishop, K., Jones, M., Li, M. et al. (2015). High-throughput gene targeting and phenotyping in zebrafish using CRISPR/Cas9. *Genome Res.* **25**, 1030-1042. doi:10.1101/gr.186379.114

Walton, E. M. (2018). Cell wall lipids promoting host angiogenesis during mycobacterial infection. *PhD thesis*, Duke University, Durham, NC.

Wang, L., Zhou, J.-y., Yao, J.-h., Lu, D.-r, Qiao, X.-j. and Jia, W. (2010). U6 promoter-driven siRNA injection has nonspecific effects in zebrafish. *Biochem. Biophys. Res. Commun.* **391**, 1363-1368. doi:10.1016/j.bbrc.2009.12.065

Wang, J., Li, X., Zhao, Y., Li, J., Zhou, Q. and Liu, Z. (2015). Generation of cell-type-specific gene mutations by expressing the sgRNA of the CRISPR system from the RNA polymerase II promoters. *Protein Cell* **6**, 689-692. doi:10.1007/s13238-015-0169-x

Wilusz, J. E., JnBaptiste, C. K., Lu, L. Y., Kuhn, C.-D., Joshua-Tor, L. and Sharp, P. A. (2012). A triple helix stabilizes the 3′ ends of long noncoding RNAs that lack poly(A) tails. *Genes Dev.* **26**, 2392-2407. doi:10.1101/gad.204438.112

Wu, J., Kent, I. A., Shekhar, N., Chancellor, T. J., Mendonca, A., Dickinson, R. B. and Lele, T. P. (2014). Actomyosin pulls to advance the nucleus in a migrating tissue cell. *Biophys. J.* **106**, 7-15. doi:10.1016/j.bpj.2013.11.4489

Xie, K., Minkenberg, B., Yang, Y. and Doudna, J. A. (2015). Boosting CRISPR/Cas9 multiplex editing capability with the endogenous tRNA-processing system. *Proc. Natl. Acad. Sci. USA* **112**, 3570-3575. doi:10.1073/pnas.1420294112

Xiong, F., Wei, Z.-Q., Zhu, Z.-Y. and Sun, Y.-H. (2013). Targeted expression in Zebrafish primordial germ cells by Cre/loxP and Gal4/UAS systems. *Mar. Biotechnol.* **15**, 526-539. doi:10.1007/s10126-013-9505-4

Yin, L., Maddison, L. A., Li, M., Kara, N., Lafave, M. C., Varshney, G. K., Burgess, S. M., Patton, J. G. and Chen, W. (2015). Multiplex conditional mutagenesis using transgenic expression of Cas9 and sgRNAs. *Genetics* **200**, 431-441. doi:10.1534/genetics.115.176917

Zhao, Z., Cao, Y., Li, M. and Meng, A. (2001). Double-stranded RNA injection produces nonspecific defects in zebrafish. *Dev. Biol.* **229**, 215-223. doi:10.1006/dbio.2000.9982

Zhou, W., Cao, L., Jeffries, J., Zhu, X., Staiger, C. J. and Deng, Q. (2018). Neutrophil-specific knockout demonstrates a role for mitochondria in regulating neutrophil motility in zebrafish. *DMM Dis. Model. Mech.* **11**, dmm033027. doi:10.1242/dmm.033027

Zhou, W., Hsu, A. Y., Wang, Y., Syahirah, R., Wang, T., Jeffries, J., Wang, X., Mohammad, H., Seleem, M. N., Umulis, D. et al. (2020). Mitofusin 2 regulates neutrophil adhesive migration and the actin cytoskeleton. *J. Cell Sci.* **133**, jcs248880. doi:10.1242/jcs.248880

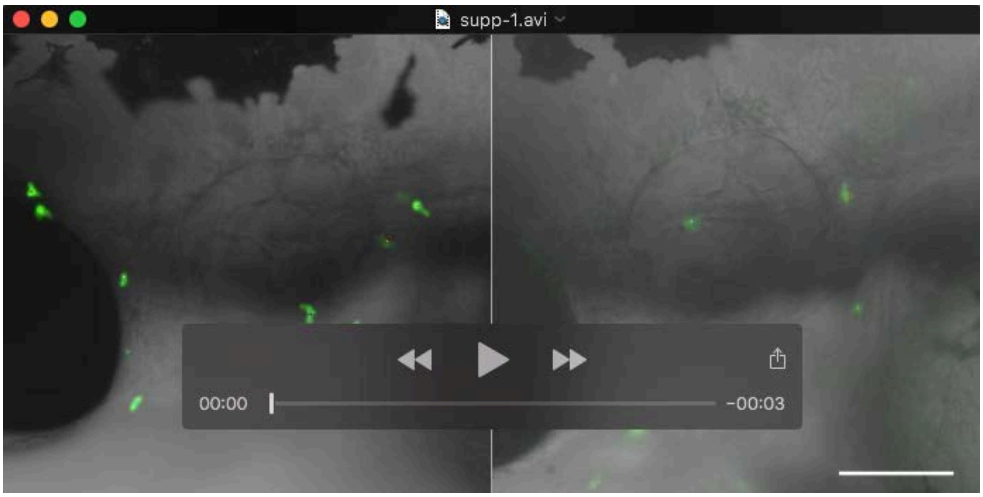

Movie 1. Tracked movies of migrating neutrophils in the head mesenchyme transiently expressing control or *rac2* sgRNAs. The video shows the motility of neutrophils in 3 dpf *Tg(lyzC:Cas9, cry:GFP)*^{pu26} zebrafish larvae injected with plasmids carrying control or *rac2* sgRNAs. Videos were recorded for 30 min with 1min interval. Representative videos from n = 3 independent experiments with 4 fish each group are shown. Scale bar: 100 µm.

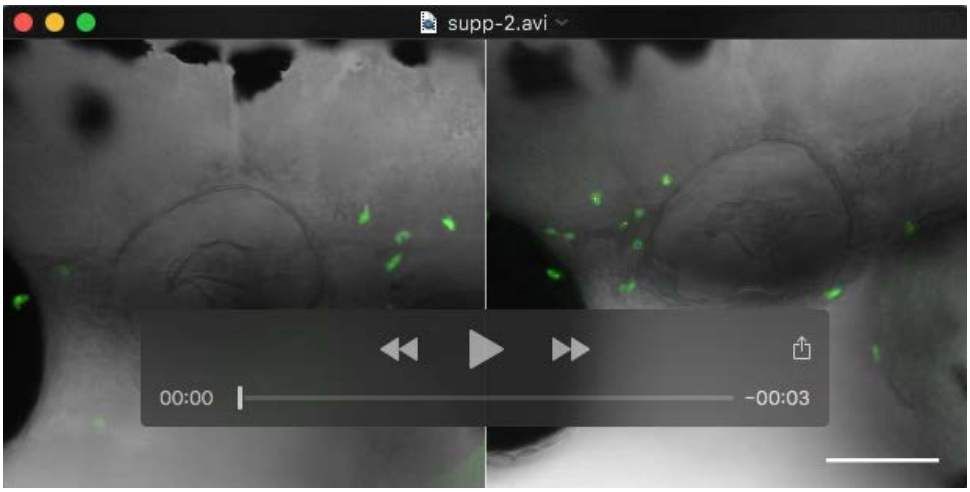

Movie 2. Tracked movies of neutrophil motility in the head mesenchyme of the control and *rac2* knockout stable lines. We generated stable lines by crossing *Tg*(*lyzC:Cas9, Cry:GFP*)^{pu26} with *Tg(u6a/c: ctrl sgRNA, lyzC:GFP)*^{pu27} or *Tg(u6a/c: rac2 sgRNA, lyzC:GFP)*^{pu28}. The video shows the motility of neutrophils in 3 dpf zebrafish offspring larvae. Videos were recorded for 30 min with 1 min interval. Representative videos from n = 3 independent experiments with 3 fish each group are shown. Scale bar: 100 µm.

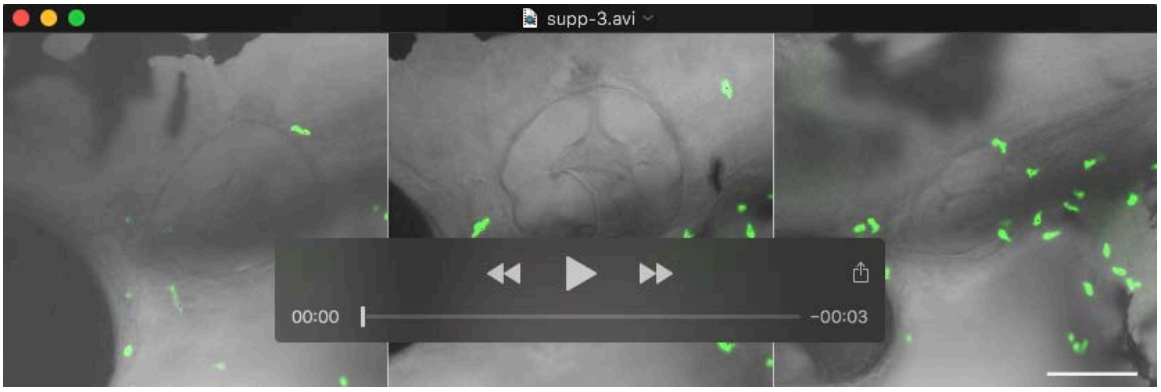

Movie 3. Tracked movies of neutrophil motility in the head mesenchyme of the no-guide control, control and *rac2* sgRNAs stable lines. The video shows the motility of neutrophils in 3 dpf zebrafish larvae of *Tg(lyzC:GFP)*, *Tg(u6a/c: ctrl sgRNA, lyzC:GFP)*^{pu27} or *Tg(u6a/c: rac2 sgRNA, lyzC:GFP)*^{pu28}. Videos were recorded for 30 min with 1 min interval. Representative videos from n = 3 independent experiments with 3 fish each group are shown. Scale bar: 100 µm.

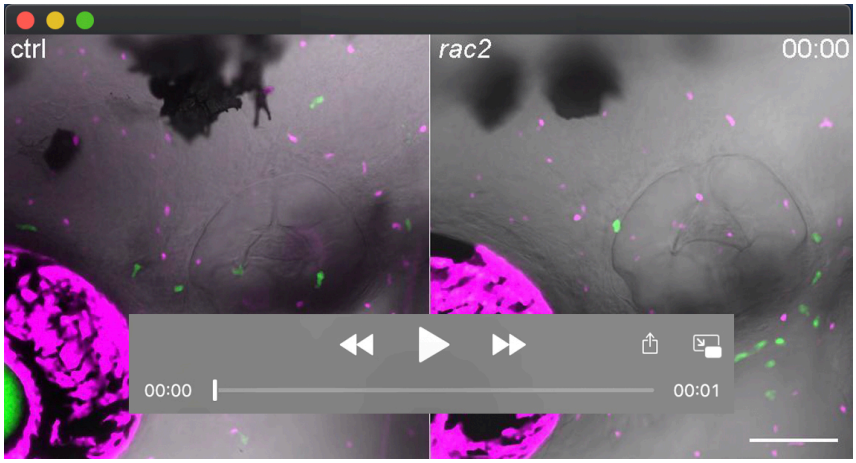

Movie 4. Tracked movies of neutrophil and macrophage motility in the head mesenchyme of the control (left) and *rac2* knockout (right) stable lines. We generated stable lines by crossing *Tg*(*lyzC:Cas9, Cry:GFP*) ^{pu26} with *Tg(u6a/c: ctrl sgRNA, lyzC:GFP, mpeg:mcherry-H2B)*^{pu27} or *Tg(u6a/c: rac2 sgRNA, lyzC:GFP, mpeg:mcherry-H2B*) ^{pu28}. The video shows the motility of neutrophils (yellow tracks) and macrophages (red tracks) in 3 dpf zebrafish offspring larvae. Videos were recorded for 90 min with 3 min interval. Representative videos from n = 3 independent experiments with 3 fish each group are shown. Scale bar: 100 µm.

Journal of Cell Science • Supplementary information

Movie 5. Tracked movies of neutrophil motility in the head mesenchyme transiently expressing *rac2*-R-WT, *rac2*-R-DN, or *rac2*-R-CA. The video shows the motility of neutrophils in 3 dpf *Tg*(*lyzC:Cas9, cry:GFP*)^{pu26} zebrafish larvae injected with plasmids carrying *rac2* sgRNAs along with *rac2*-R-WT, *rac2*-R-DN, or *rac2*-R-CA. Videos were recorded for 30 min with 1 min interval. Representative videos from n = 3 independent experiments with 3 fish each group are shown. Scale bar: 100 µm.

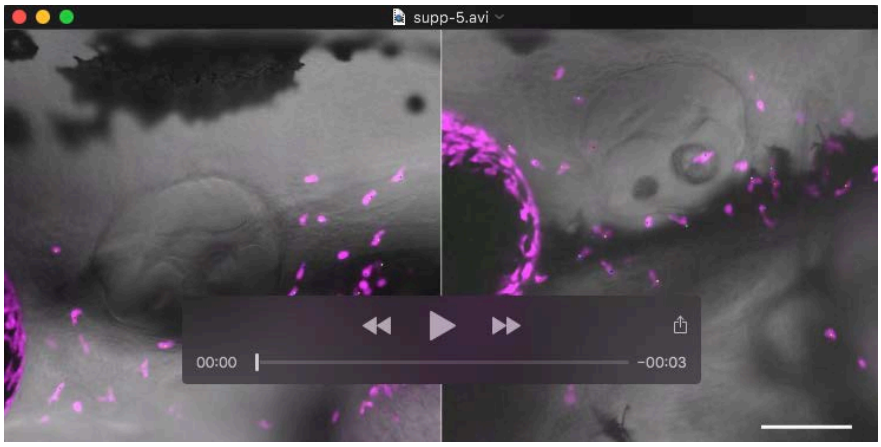

Movie 6. Migrating neutrophils in the head mesenchyme of the *rac2*-CA and the *rac2*-CA lines. The video shows the motility of neutrophils in 3 dpf *Tg*(*lyzC:rac2-WT-2a-mcherry*)^{pu30} or *Tg(lyzC:rac2-CA-2a-mcherry)*^{pu29} zebrafish larvae. Videos were recorded for 30 min with 1 min interval. Representative videos from n = 3 independent experiments with 3 fish each group are shown. Scale bar: 100 µm.

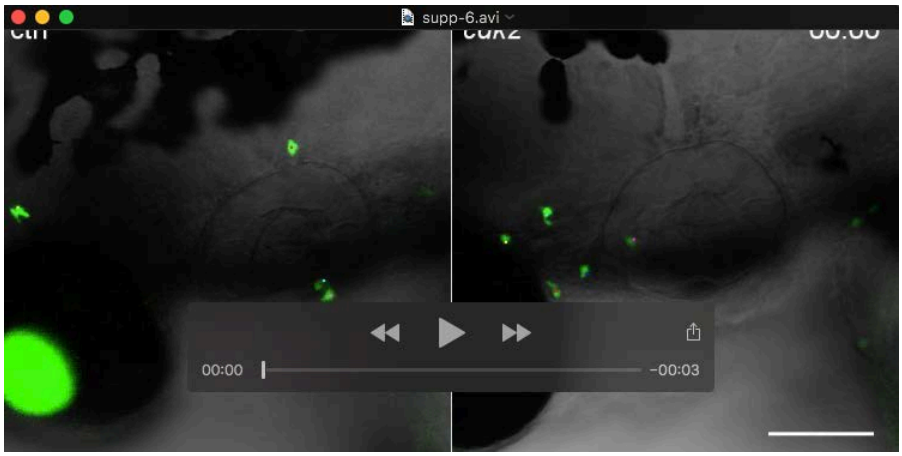

Movie 7. Tracked movies of migrating neutrophils in the head mesenchyme transiently expressing control or *cdk2* sgRNAs. The video shows the motility of neutrophils in 3 dpf Tg(*lyzC:Cas9, cry:GFP*)^{pu26} zebrafish larvae injected with plasmids carrying control or *cdk2* sgRNAs. Videos were recorded for 30 min with 1 min interval. Representative videos from n = 3 independent experiments with 3 fish each group are shown. Scale bar: 100 µm.

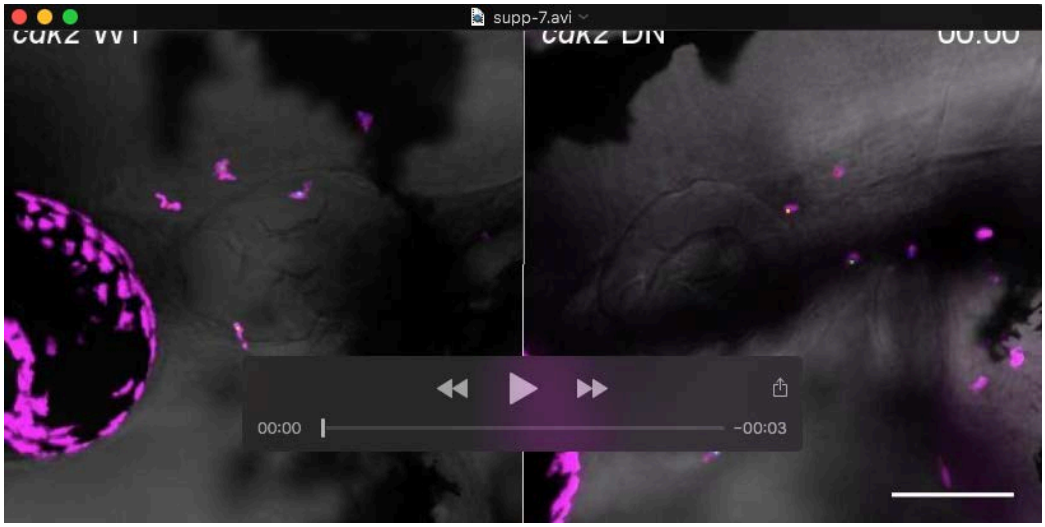

Movie 8. Transient expression of *cdk2*-R-WT, not *cdk2*-R-DN, restored cell motility in *cdk2*-deficient neutrophils. The video shows the motility of neutrophils in 3 dpf *Tg*(*lyzC:Cas9, cry:GFP*)^{pu26} zebrafish larvae injected with plasmids containing *cdk2* sgRNAs along with *cdk2*-R-WT or *cdk2*-R-DN. Videos were recorded for 30 min with 1 min interval. Representative videos from n = 3 independent experiments with 3 fish each group are shown. Scale bar: 100 μm.

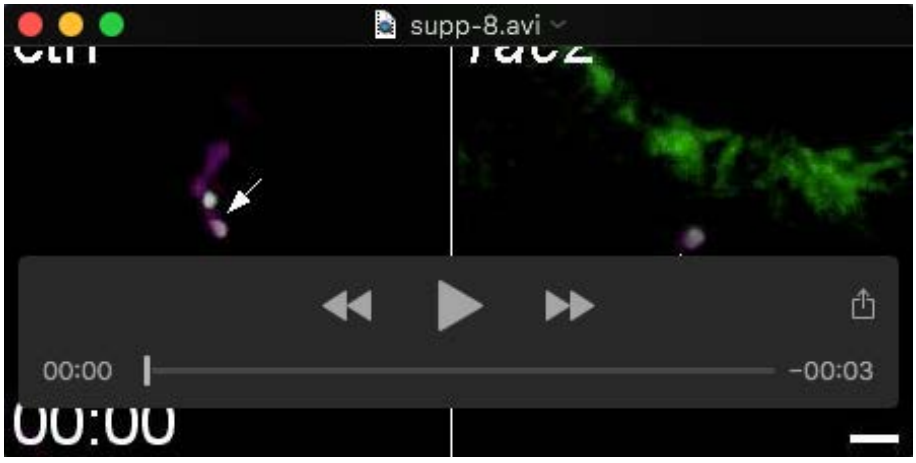

Movie 9. Neutrophil-specific *rac2* knockout lead to deficiency in the front-to-rear localization of Rac in neutrophils. The video shows the subcellular localization of PBD-GFP, which marks the location of Rac in neutrophils of 3 dpf *Tg*(*lyzC:Cas9, cry:GFP*)^{pu26} zebrafish larvae injected with plasmids containing control or *rac2* sgRNAs. Cytoplasm is labeled with mCherry. Scale bar: 20 μm.

Movie 10. Neutrophil-specific *rac2* knockout abolished the oscillation between the front and rear of active Rac in neutrophils. The video shows the subcellular localization of Rac-FRET, of which the YFP/CFP fluorescence ratio indicates the location of active Rac in neutrophils of 3 dpf *Tg(lyzC:Cas9, cry:GFP)*^{pu26} zebrafish larvae injected with plasmids containing control or *rac2* sgRNAs. Scale bar: 10 μm.

Movie 11. Neutrophil-specific *rac2* knockout induced stable F-actin changes in neutrophils. The video shows neutrophils expressing GFP-UtrCH, which labels stable F-actin, along with control or *rac2* sgRNAs in 3 dpf *Tg(lyzC:Cas9, cry:GFP)*^{pu26} zebrafish larvae. Cytoplasm is labeled with mCherry. Scale bar: 20 μm.

Movie 12. Neutrophil-specific *rac2* knockout abrogated the generated actin stress at the front and the back. The video shows neutrophils expressing AcpA-FRET along with control or *rac2* sgRNAs in 3 dpf *Tg(lyzC:Cas9, cry:GFP)*^{pu26} zebrafish larvae. The ratiometric AcpA-FRET signals report the actin force in neutrophils. Scale bar: 100 µm.

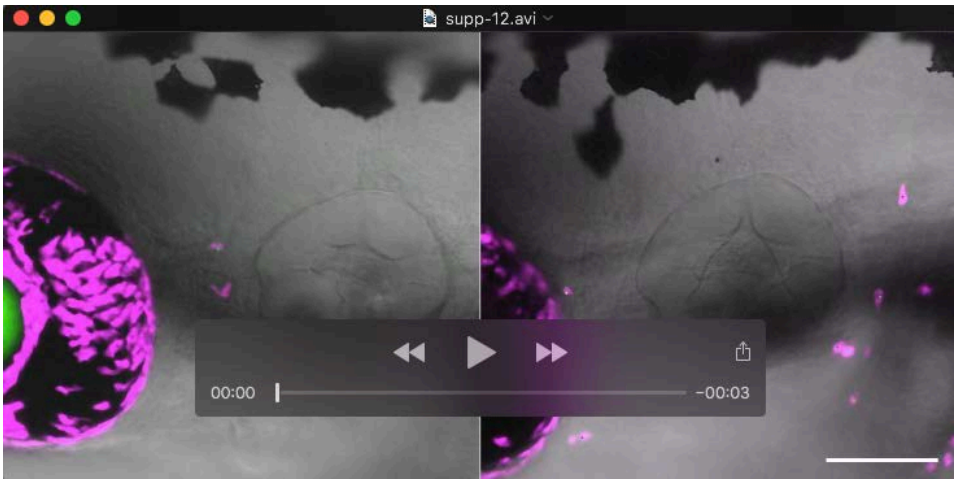

Movie 13. Tracked movies of migrating neutrophils in the head mesenchyme transiently expressing control or *rac2* sgRNAs. The video shows the motility of neutrophils in 3 dpf *Tg(ubb:cas9, cry:GFP)*^{xt48} zebrafish larvae injected with plasmids carrying Ribozyme-processing machinery along with the control or *rac2* sgRNAs. Videos were recorded for 30 min with 1 min interval. Representative videos from n = 3 independent experiments with 3 fish each group are shown. Scale bar: 100 µm.

Movie 14. Tracked movies of migrating neutrophils in the head mesenchyme of zebrafish transiently expressing the neutrophil specific RFP with or without control or *rac2* sgRNAs. The video shows the motility of neutrophils in 3 dpf wide-type AB zebrafish larvae transiently expressing RFP with or without control sgRNA or *rac2* sgRNA in neutrophils. Videos were recorded for 30 min with 1 min interval. Representative videos from n = 3 independent experiments with 4 fish each group are shown. Scale bar: 100 μm.

Table S1. Oligo design template tool for ribozyme sgRNAs

Click here to download Table S1